



REPUBLIC OF TURKIYE
ALTINBAŞ UNIVERSITY
Institute of Graduate Studies
Mechanical Engineering

**THERMAL ANALYSIS OF PCM WITH GLASS
FOR INSULATION APPLICATIONS IN
TURKIYE**

Ramadan Ali Mohamed Salim ELFAITURI

Master of Science

Supervisor

Assoc. Prof. Dr. Süleyman BAŞTÜRK

Istanbul, 2022

**THERMAL ANALYSIS OF PCM WITH GLASS FOR INSULATION
APPLICATIONS IN TURKIYE**

Ramadan Ali Mohamed Salim ELFAITURI

Mechanical Engineering

Master of Science

ALTINBAŞ UNIVERSITY

2022

The thesis titled THERMAL ANALYSIS OF PCM WITH GLASS FOR INSULATION APPLICATIONS IN TURKIYE prepared by RAMADAN ALI MOHAMED SALIM ELFAITURI and submitted on 19/08/2022 has been **accepted unanimously** for the degree of Master of Science in Mechanical Engineering.

Assoc. Prof. Dr. Süleyman BAŞTÜRK

Supervisor

Thesis Defense Committee Members:

Assoc. Prof. Dr. Süleyman
BAŞTÜRK

Faculty of Engineering
and Architecture,
Altinbas University

Asst. Prof. Dr. Serdar AY

Faculty of Engineering
and Architecture,
Altinbas University

Asst. Prof. Dr. Haydar UYANIK

College of Applied
Sciences
KTO Karatay University

I hereby declare that this thesis meets all format and submission requirements of a master's thesis.

Submission date of the thesis to Institute of Graduate Studies: __/__/__

I hereby declare that all information/data presented in this graduation project has been obtained in full accordance with academic rules and ethical conduct. I also declare all unoriginal materials and conclusions have been cited in the text and all references mentioned in the Reference List have been cited in the text, and vice versa as required by the abovementioned rules and conduct.

Ramadan Ali Mohamed Salim Elfaituri

DEDICATION

Thank you, Allah.

I'd want to express my gratitude to my first professors, my family, who served as my initial role models and supports along the journey, as well as my wife. If it wasn't for you, this dream would never have come true.



PREFACE

I'd want to express my gratitude to everyone who has supported me along this long and winding trip. I'd want to thank Assoc. Prof. Dr. Süleyman BAŞTÜRK, my supervisor, for keeping me on track even when I believed I was lost and for being an integral part of the effort's summit. I'd also want to thank my supervisor for his supportive remarks, which helped to increase the quality of this project greatly. Finally, I'd want to express my gratitude to this institution for welcoming me throughout the years and firmly establishing itself as a member of my family. I am thankful to my family, whose views and education motivate me to ask questions about my relatives and family's unconditional love; and to my country, which, despite its many flaws, continues to inspire me to ask questions.

ABSTRACT

THERMAL ANALYSIS OF PCM WITH GLASS FOR INSULATION APPLICATIONS IN TURKIYE

Elfaituri, Ramadan Ali Mohamed Salim

M.Sc., Mechanical Engineering, Altınbaş University,

Supervisor: Assoc. Prof. Dr. Süleyman BAŞTÜRK

Date: August/2022

Pages: 61

Nowadays, increasing insulation efficiency and decreasing energy consumption are fundamental factors to enhance the thermal performance of the double glass unit. A parametric CFD study was conducted numerically for various thicknesses on the insulation performance using ANSYS Fluent software on the hottest day in Adana in Türkiye. Four PCM layer thicknesses were investigated such as 6 mm, 10 mm, 15 mm, and 20 mm. The mesh was generated and verified then the results were validated with previous data, and a good agreement has been reached. The results revealed that as the PCM layer thickness increased, the external outer glass temperature decreased, with the 20 mm thickness achieving the lowest external temperature. In the case of a PCM layer with a thickness of 6 mm, the PCM layer began to melt at 7:00 a.m. for a few hours until it reached full melting, after which solidification proceeded until the PCM layer was entirely solidified at 11:00 p.m. The mass fraction distribution for a 10 mm thickness is chosen since it is the best option for unit performance. The middle part of the PCM layer showed the least overall deformation, whereas the edges of the glass layers showed the most. Therefore, the thickness from 10 mm to 15 mm is the optimum choice for the advantages of the smallest temperature.

Keywords: Phase Change Material, Finite Element Analysis, Double Glazing Unit.

TABLE OF CONTENTS

	<u>Pages</u>
ABSTRACT	vii
LIST OF TABLES.....	x
LIST OF FIGURES.....	xi
ABBREVIATIONS.....	xiii
LIST OF SYMBOLS.....	xiv
1. INTRODUCTION.....	1
1.1 THERMAL INSULATION	1
1.2 INSULATION IN BUILDINGS	1
1.3 COMMON MATERIALS FOR INSULATIONS	2
1.3.1 Fiberglass Insulation	2
1.3.2 Properties Of Fiberglass Insulation	2
1.3.3 Mineral Wool	3
1.3.4 Cellulose.....	4
1.3.5 Polyurethane Foams	5
1.3.6 Polystyrene.....	5
1.4 THERMAL RESISTANCE OF INSULATION MATERIALS	6
1.5 PHASE CHANGE MATERIAL (PCM).....	8
1.5.1 PCM Advantage	8
1.5.2 PCM Disadvantages	9
2. LITERATURE REVIEW.....	10
2.1 INTRODUCTION.....	10
2.2 THE NOVELTY OF THE STUDY	22
3. NUMERICAL STUDY	24

3.1	PHYSICAL DOMAIN.....	24
3.2	MESH GENERATION.....	27
3.3	GOVERNING EQUATIONS.....	28
3.4	COST ANALYSIS.....	31
4.	RESULTS AND DISCUSSIONS	34
4.1	MODEL VALIDATION.....	34
4.2	TEMPERATURE AND MASS FRACTION	35
4.3	STRESS ANALYSIS FOR GLASS LAYER AND PCM LAYER.....	43
4.4	COST RESULTS	45
5.	CONCLUSIONS.....	48
	REFERENCES	50

LIST OF TABLES

	<u>Pages</u>
Table 1.1: Properties of Polystyrene [1].....	6
Table 1.2: Properties of Insulation Materials [1].....	7
Table 3.1: The thermal properties of the PCM material and glass layer.	25
Table 3.2: The optical properties of the PCM material and glass layer.	25
Table 4.1: Summary of the results.....	47

LIST OF FIGURES

	<u>Pages</u>
Figure 1.1: Fiberglass Insulation material [1].	3
Figure 1.2: Mineral Wool material [1].	4
Figure 1.3: Cellulose material [1].....	5
Figure 2.1: Influence of the aspect ratio of annular space on the solidification time [3]......	11
Figure 2.2: Superficial and PCM temperature course for panel configuration [6].....	13
Figure 2.3: Heat flux at the indoor surface for different PCMs [9].....	15
Figure 2.4: Seasonal energy savings as a function of PCM layer thickness [21].....	19
Figure 2.5: Highest peak heat flux decreases for numerous PCM layer thicknesses as a function of PCM phase change temperature and a greatest wall surface temperature of 70 °C [23].	21
Figure 3.1: Modelling of PCM with glass unit.....	24
Figure 3.2: Glass layers with PCM layer and heat transfer mechanisms.	26
Figure 3.3: Various thickness of PCM layer (a) 6 mm (b) 10 mm (c) 15 mm (d) 20 mm.	26
Figure 3.4: Three dimensions and side view of mesh grids.	27
Figure 3.5: Ambient temperature in Adana city on 29 July 2020 [25].....	30
Figure 3.6: Solar radiation in Adana city on 29 July 2020 [25].	31
Figure 4.1: Comparing the numerical results of external temperature with a previous experimental study [29].....	35
Figure 4.2: External temperature of outer glass for different thicknesses of PCM layer.	36
Figure 4.3: Mass fraction of PCM layer for different PCM layer thicknesses.....	37

Figure 4.4: Total transmitted energy versus time.....	38
Figure 4.5: Temperature distribution of glass unit and PCM layer at 10 pm for various thicknesses such as a)6 mm, b)10 mm, c)15 mm, and d)20 mm.....	39
Figure 4.6: Temperature distribution of inner glass layer at 10 pm for various thicknesses such as a)6 mm, b)10 mm, c)15 mm, and d)20 mm.	39
Figure 4.7: Temperature distribution of PCM layer at 10 pm for various thicknesses such as a)6 mm, b)10 mm, c)15 mm, and d)20 mm.....	40
Figure 4.8: Temperature distribution of external glass layer at 10 pm for various thicknesses such as a)6 mm, b)10 mm, c)15 mm, and d)20 mm.....	40
Figure 4.9: Mass fraction distribution at 12 pm for various thicknesses such as a)6 mm, b)10 mm, c)15 mm, and d)20 mm.	41
Figure 4.10: Temperature distribution for 10 mm thickness at various times a) 10:00 am, b) 2:00 pm, c) 5:00 pm, and d) 9:00 pm.	42
Figure 4.11: Mass fraction for 10 mm thickness at various times a)10:00 am, b)2:00 pm, c)5:00 pm, d)9:00 pm.	43
Figure 4.12: Equivalent stress for the glass unit with PCM layer.	44
Figure 4.13: Total deformation for the glass unit and PCM layer.....	45
Figure 4.14: PCM cost, natural gas cost, and total cost versus the PCM layer thickness.	46

ABBREVIATIONS

PCM	:	Phase Change Material
CFD	:	Computational Fluid Dynamics
FEM	:	Finite Element Method
EPS	:	Extended Polystyrene
HVAC	:	Heating Ventilation and Air Conditioning
CAD	:	Computer-Aided Design
PWF	:	Permanent Wood Foundation.
DGP	:	Daylight Glare Probability

LIST OF SYMBOLS

ψ	: radiative source, W/m^3
H	: Enthalpy, J/kg
ρ	: Density, kg/m^3
T	: Temperature, $^{\circ}\text{C}$
C_p	: Specific Heat Capacity, $\text{J}/\text{kg}\cdot^{\circ}\text{C}$
h	: The Heat Transfer Coefficient of The Internal Surface, $\text{W}/\text{m}^2\cdot\text{K}$
σ	: The Stefan–Boltzmann Constant, $\text{W}/\text{m}^2\cdot\text{K}^4$
ε	: Surface Emissivity
q_r	: Heat Transferred by Radiation, W/m^2
β	: PCM Liquid Fraction
Q_l	: Latent Heat, J/kg
T	: Temperature, K
K	: Thermal Conductivity, $\text{W}/\text{m}\cdot\text{K}$
t	: Time, s

1. INTRODUCTION

1.1 THERMAL INSULATION

Thermal insulation is the reduction of heat transfer (the flow of thermal energy between things with differing temperatures) between objects that are in thermal contact or within a radiation field. Thermal insulation can be achieved using specifically specialized technologies or procedures in addition to the appropriate item shapes and materials. Heat will always travel through objects that are in contact when their temperatures are different. Thermal insulation creates a heat barrier or break, and the lower-temperature body in this area of insulation reflects thermal radiation rather than absorbing it. The insulating power of a substance is calculated using the inverse of thermal conductivity. Low heat conductivity is equivalent to high insulating capacity (resistance value). Product density and specific heat capacity are two additional crucial insulating material characteristics in thermal engineering.

1.2 INSULATION IN BUILDINGS

Keeping buildings at comfortable temperatures requires using a lot of energy worldwide, such as for heating and cooling. As mentioned above, the concept of microscopic, trapped air cells is utilized by a variety of building insulations, including fiberglass, vermiculite, perlite, cork, rock wool, polystyrene, and urethane. Even though asbestos has detrimental impacts on health, it was used for a long. To lessen heat loss in the winter and solar heat gain in the summer, windows can be weatherized with insulating film. When a structure is properly insulated, it uses less energy to stay cool in the summer or warm in the winter. Rising energy efficiency will result in lower carbon emissions. Because the temperature is consistent across the area, it is more enjoyable. When the outside temperature is extremely cold or hot, there is less temperature differential between ankle height and head height as well as between exterior walls, ceilings, and windows and inside walls, making the environment more comfortable. In an industrial setting, energy is required to raise, reduce, or maintain an object's or a process fluid's temperature. The procedure requires more energy if these aren't insulated, increasing the cost and environmental impact.

1.3 COMMON MATERIALS FOR INSULATIONS

There are many readily available, affordable, and everyday insulating materials on the market today. Many of these have been in existence for a while. These insulating materials each have advantages and disadvantages. Someone must consider which insulating material will perform best for your circumstances when choosing which one to utilize. The top 5 types of insulating materials are listed below:

1.3.1 FIBERGLASS INSULATION

Fiberglass insulation is the most popular kind in use today. Due to the method used to make it, which involves weaving fine glass strands into an insulating layer as shown in Figure 1.1, fiberglass can reduce heat transmission. The greatest drawback of fiberglass is the risk of harm when using it. As a result of the tightly woven silicon fibers that make up fiberglass, glass powder and tiny glass shards are produced. The eyes, lungs, and even the skin could be harmed if the required safety equipment is not used. However, fiberglass installation can be done safely if the appropriate safety measures are taken.

1.3.2 PROPERTIES OF FIBERGLASS INSULATION

The thermal and mechanical properties of fiberglass can be concluded in those points:

- a. Fiberglass has a higher specific resistance than steel in terms of mechanical strength. In order to create high-performance
- b. Electrical properties: Even at modest thicknesses, fiberglass is a good electrical insulator.
- c. Because it is made of minerals, fiberglass is naturally incombustible. A flame cannot continue or expand as a result. It doesn't emit smoke or dangerous compounds when heated.
- d. Dimensional stability: Fiberglass withstands variations in temperature and humidity. It has a low coefficient of linear expansion.

- e. Fiberglass's capacity to interact with numerous synthetic resins and several mineral matrices, such as cement, and can come in a variety of sizes.
- f. Non-rotting: Fiberglass is resistant to rodent and insect damage and does not rot.
- g. Thermal conductivity: Fiberglass has a low thermal conductivity, which makes it very advantageous in the construction sector.
- h. Fiberglass has the dielectric permeability feature, which makes it excellent for electromagnetic windows.



Figure 1.1: Fiberglass Insulation material [1].

1.3.3 MINERAL WOOL

Several insulating materials are referred to as mineral wool. To begin with, it might be referring to glass wool, a kind of fiberglass manufactured from reclaimed glass. Second, it might have something to do with rock wool, a type of basalt insulation that can be seen in Figure 1.2. Lastly, it might be alluding to slag wool, which is made from steel mill slag. The majority of mineral

wool produced in the US is slag wool. Mineral wool comes in two main forms: batts and loose. Since most mineral wool doesn't have the elements needed to make it fire resistant, it can't be used in highly hot conditions. Mineral wool may be an efficient approach for insulating large spaces when used in conjunction with other, more fire-resistant types of insulation. Mineral wool insulation is advised for high-temperature situations where polymer coatings are not considered appropriate. Densities of mineral wool typically range from 120 to 140 kg/m³. Thermal conductivity measurements on mineral wool typically range from 30 to 40 mW/mK. Mineral wool's heat conductivity is influenced by temperature, moisture content, and mass density in many ways. As an example, the heat conductivity of mineral wool may increase from 37 to 55 mW/mK as its moisture content increases from 0 to 10%, respectively. Materials made of mineral wool can be cut, pierced, and manipulated without losing any of their thermal resistance on the job site.



Figure 1.2: Mineral Wool material [1].

1.3.4 CELLULOSE

Cellulose insulation is one of the greenest types of insulation. Cellulose is a loose substance made from recycled cardboard, paper, and other like materials. Due to its tight structure, cellulose has a relatively low oxygen concentration. By removing the substance's oxygen, this

helps to reduce the possible harm that a fire could do. Because of this, cellulose is one of the most environmentally friendly and fire-resistant insulation materials available.



Figure 1.3: Cellulose material [1].

1.3.5 POLYURETHANE FOAMS

Despite not being the most popular type of insulation, polyurethane foams are really a decent choice. Polyurethane foams are now blown with non-chlorofluorocarbon gas. This lessens the amount of harm that is done to the ozone layer. They weigh only two pounds per cubic foot, which is not particularly heavy. Their resistance R-value per inch of thickness is around 3.6. In locations lacking insulation, low density foams may also be sprayed. R-3.6 is a standard rating for this type of polyurethane insulation per inch of thickness. Another benefit of this kind of insulation is its fire resistance. The ultimate and yield tensile strengths of polyurethane range from 0.0207 to 1900 MPa and 0.0814 to 103 MPa, respectively, while its hardness ranges from 10.0 to 45.0. The elastic modulus is measured between 0.000138 and 3.45 GPa.

1.3.6 POLYSTYRENE

A thermoplastic, waterproof substance that insulates sound and temperature is polystyrene. The two types are commonly referred to as Styrofoam and are expanded (EPS) and extruded (XEPS). The two variations have differing cost and performance ratings. EPS has an R-value of R-4 while the more expensive XEPS has an R-value of R-5.5. The forms of insulation cannot

compare to the smooth surface of polystyrene insulation. Table 1.1 provides an illustration of Polystyrene's characteristics.

Table 1.1: Properties of Polystyrene [1]

Property	Value	unit
Density	1070	kg/cm ³
Hardness of the Surface	RM80	
Tensile Strength	34	MPa
Flexural Modulus	3	GPa
Elongation at Break	1.6%	
Strain at Yield	1.4%	°C
Maximum Operating Temperature	50	
Absorption of Water	0.05%	°C
Oxygen Index	18%	°C
Melting Temperature Range	200-250	°C
Mould Shrinkage	0.5%	
Mould Temperature Range	20-50	

1.4 THERMAL RESISTANCE OF INSULATION MATERIALS

The thermal resistance (R) is defined by the material thickness and the temperature. In basic words, the R-value is the resistance that a particular material provides the heat flow. The R-value of suitable insulating material should be high. To lower the overall coefficient of heat transmission, the best insulating materials must get the smallest thermal conductivity. As a result, less insulation material will be needed. One of the greatest insulating materials is dry stagnant gas. The volume of gas trapped within the substance and the quantity of gas compartments dictates the insulating qualities of commercially available insulating materials. As a result, the thermal conductivity of such as isolating material decreases as the number of

cells and their size increase. These cells would not be interconnected since this permits heat to transfer. The thermal properties of common insulation materials are demonstrated in Table 1.2.

Table 1.2: Properties of Insulation Materials [1]

Fiber	Diameter (μm)	Density (g/cm^3)	Moisture (%)	UTS⁻¹ MPa	Modulus GPa
Cotton		1.5		500-880	0.05
Jute	200	1.45	12	460-533	2.5-13
Coir	100-450	1.15	10-12	131-175	4-6
Banana	80-250	1.35	10-12	529-754	7.7-20.8
Sisal	50-200	1.45	11	568-640	9.4-15.8
Flax		1.50		1100	100
Kraft fiber		1.54		1000	40
Sunhemp	48	0.673		200-300	2.68
Pineapple	20-80	1.44		413-1627	34.5
Palm leaf	240			98.14	2.22
Mesta	200	1.47		157.38	12.62
Kusha grass	390			150.59	5.69

Reduced heat transmission via the walls, hatches, pipes, and stanchions of the fish hold into the area used to keep chilled fish is the primary objective of the thermal insulation materials used in small ice-fishing vessels. The efficiency of the icing process can be increased by limiting heat loss, which will decrease the amount of ice that melts. As was previously stated, ice is consumed because it absorbs heat energy from the fish as well as heat energy that escapes through the walls of the storage container. By insulating the container's walls to lessen the amount of heat

that enters the container, the amount of ice required to keep the contents cool can be decreased. Reducing heat transmission from warm air surrounding it, the fuel tank, and heat leaks such fish hold wall surfaces, entryways, pipes, and stanchions are the main benefits of efficiently insulating the fish hold. The fish hold's beneficial capacities are also increased, fish-chilling operation expenses are decreased, and, if refrigeration systems are used, energy requirements for these systems are decreased.

1.5 PHASE CHANGE MATERIAL (PCM)

During a phase transition, PCM is a material that may emit or absorb enough energy to provide useful heat or cooling. Most of the time, the change will occur between the solid or the liquid, the initial two basic states of matter. The phase transition can also happen between forms of matter that are not classified as classical, a transition from one type of crystalline structure to another that may have a higher or lower energy state, as in crystal conformity. The energy created or absorbed as a solid transform into a liquid, or vice versa is known as the heat of fusion and is typically far higher than the heat that can be felt. In contrast to sensible heat storage, a PCM may absorb and release huge amounts of energy by melting and solidifying at the phase transition temperature. Because energy is absorbed or released as a material change from solid to liquid or vice versa, or when its micro-structural changes, PCMs are also known as latent heat storage materials.

1.5.1 PCM Advantage

PCMs have various advantages when they are employed in products. They include better cooling and heating in distant regions without access to power, better electronic performance, better sleep, and energy savings. Here are just a few of the many advantages of PCM materials:

- a. Phase change temperature within necessary limits with distinct melting and freezing spots and high latent heat of fusion
- b. Does not react with other substances and functions as a solvent for packaging materials.
Landfill throwaway and waterway not reusable

- c. Biodegradable, non-flammable, and disposable for landfills and waterways, with a high flash point and low vapor pressure
- d. Corrosiveness
- e. Available at a small cost
- f. Limited volumetric expansion and contraction upon freeze and thaw
- g. Stability upon thermal cycling without supercooling

1.5.2 PCM DISADVANTAGES

Corrosiveness, instability, poor resolidification, and a propensity to overcool are a few of these drawbacks. Salt hydrate materials have a high storage density, which is challenging to maintain and typically drops with cycling. The following list of PCM material's drawbacks can be drawn to a conclusion:

- a. Compatibility
- b. Packaging for Purpose
- c. Material Properties as well as Thermal Performance
- d. Preparing for Use
- e. Price and Accessibility
- f. Health and Safety

2. LITERATURE REVIEW

2.1 INTRODUCTION

Using PCM with glass is a practical solution to reduce building energy use and maximize solar energy use, which enhances the thermal performance of the glazing. An element called PCM emits or absorbs enough energy to provide considerable heating or cooling at the phase shift. Typically, a change would occur from one of the two main states of matter, such as solid or liquid, to the other. Phase transitions between non-traditional matter situations, such as crystal conformity, may occur as the raw material transforms from one crystalline form to another, each of which may have a different level of energy.

Ismail and Gonçalves [2] proposed a phase change two-dimensional model, conduction established by the heat transfer about a cylinder absorbed in the PCM. The conclusions indicated the influences of the modification of the internal to external radius ratio, Stefan number, Biot number, employed fluid intake temperature, and efficacy of frozen mass fraction.

A computer simulation of PCM solidification in a sphere-shaped shell was provided by Ismail and Henriquez [3]. The model depends on either heat transmission via convection on the surface of the spherical shell or conduction of the PCM at a constant temperature. The model was validated by comparing it to other similar models that were already accessible, and the agreement was judged to be adequate. The model was then utilized to forecast the solidified mass percentage and duration for complete solidification based on the spherical shell sizes, shell thicknesses and materials, beginning PCM temperatures, and exterior wall surface temperature.

Ismail et al. [3] used computational and experimental methods to examine finned tubes in thermal storage devices. The findings supported the fins' relevance in postponing the negative impacts of natural convection during phase transitions. The size of the annulus space, radially fin length, and a number of fins have a big impact on the consolidated mass fraction and overall phase shift duration. A metallic tube with four or five fins of uniform thickness equal to the tube wall thickness and radial length roughly twice the tube diameter should be a compromise between efficiency, increase in heat flow rate, and loss of available storage capacity, according

to empirical findings and computational results. Figure 2.1 illustrates the relationship between the annular space's aspect ratio and solidification time.

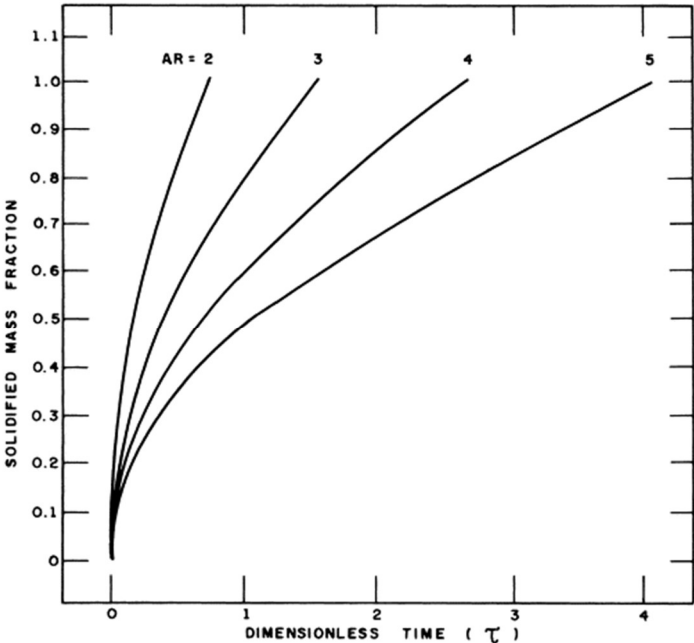


Figure 2.1: Influence of the aspect ratio of annular space on the solidification time [3].

Cabeza et al. [5] investigated three methods, including the insertion of stainless-steel bits, copper bits, and a unique PCM-graphite composite material, to enhance heat transmission in cold storage utilizing water and ice as the PCM. Compared to other techniques, the PCM-graphite composite material showed a larger rise in heat flow.

Ismail and Henriquez [4] demonstrated a mathematical model of heat transport over a simple glass window with numerical simulations. In the numerical simulations, variable cases of solar energy and ambient outside temperature were taken into account. It is stated that numerical simulations were carried out for absorbing and pure glasses to demonstrate the impact of glasses width on solar heat gain, whole heat gain, and shading factor.

Koschenz et al. [5] spoke about the creation of a thermal-actuated ceiling control panel for use in insubstantial and retrofitting structures. The new ceiling panel's design takes advantage of the

capabilities of paraffin, a PCM. A combined water capillary tubes scheme was used to actively manage the heat storage. The creation of a simulation model for calculating the walls as well as ceiling system's thermal behavior integrating PCMs was also part of the research effort. To calculate the requisite thermal characteristics of the ceiling panels and define specifications for the used materials, simulation computations were undertaken. To validate the system's performance, laboratory experiments were conducted, and a pilot application will be tested in the near future.

Quantitative research on the effectiveness of PCM as a pipe thermal insulation was done by Alawadhi et al. [8]. The effectiveness of the PCM insulation was assessed by contrasting its thermal performance with that of insulation with no phase change. Both time-dependent and time-independent boundary conditions were studied. In the time-independent scenario, the PCM insulation reduces the heat loss from the pipe over a significant time if the Rayleigh number was low. Regarding the time-dependent example, PCM insulation effectively lowers heat loss for a sizable amount of time. Both the flow structural features and the high-resolution capture of the solid/liquid flowing border were displayed.

Carbonari et al. [9] examined four models of PCM sandwich panels for pre-fabricated walls in a test chamber that simulated a variety of indoor and outdoor climate factors in order to evaluate the energetic performance results of those panels, which make them appealing for use during various climatic situations or numerous architectural details. They can be installed on walls, ceilings, and in a variety of climatic and architectural settings, as illustrated in Figure 2.2 because it is possible to modify such basic technology to produce panels with various stratifications.

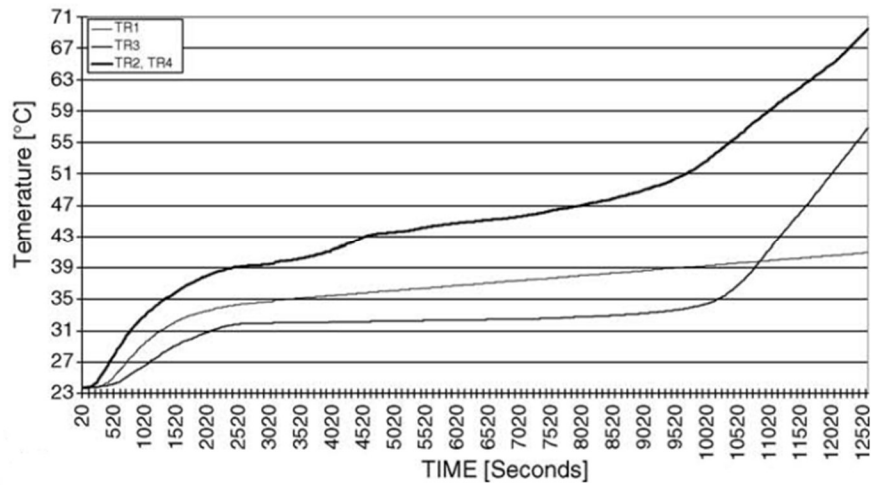


Figure 2.2: Superficial and PCM temperature course for panel configuration [6].

Cabeza et al [10] completed an investigation on the thermal characteristics of a novel, ground-breaking concrete that contains PCMs. The final objective was to develop a product that would significantly reduce the amount of energy used by buildings. In order to research the consequences of including a PCM with a melting point of 26 degrees Celsius, the project entailed fabricating and installing investigative equipment in two full-volume concrete cubicles. According to the study's findings, embedding PCMs in the walls stores energy, which increases thermal inertia and lowers interior temperatures when compared to concrete which doesn't include PCMs.

In a heated setting, Ismail et al. [11] investigated the thermal performance of two glass walls—one with a PCM and the other with an absorbing gas—due to solar radiation. An IR-absorbing double glass window was modeled using a continuous-wave real gas model. Both a radiation-conducting model and radiative convection conducting model were examined by the researchers. The researchers used a mixture of pure infrared radiation, a mixture of infrared radiation with low absorption, and a mixture of infrared radiation with high absorption. A double glass window loaded with a PCM was explained using a fairly quick and straightforward one-dimensional radiative conduction equation.

Castellón et al. [7] put his PCM experimental setup to the test in real-world situations, using a variety of standard insulation and building materials. Two concrete, five ordinary bricks, and two alveolar bricks were used to build nine tiny house-sized cubicles. The PCM cubicle's peak temperatures were moved to later hours, and temperature oscillation was reduced by up to 4°C, so the concrete cubicles' results remained excellent. By using PCM at set points greater than 20°C throughout the summer, the HVAC system in the brick cubicles used less energy. Wintertime cubicle temperatures are kept warmer by the PCM's insulating effect, especially during the chillier hours of the day.

Miller et al. [8] studied variable styles of PCMs as dynamic parts. PCMs have been proven to improve building energy efficiency in the majority of research conducted in the past. PCM-improved construction materials, such as gypsum boards and impregnated concretes, have seen partial use in various nations. The addition of roughly 20 wt% PCM in the insulation resulted in a 30 % decrease in heat flow in laboratory tests. To provide energy performance data for different US climates, the investigational study was monitored by thorough total building Energy Plus simulations. Furthermore, a sequence of numerical models and area testing revealed the potential for new insulation of PCM fiber glasses to be used as an allowing technological through Attica thermal improvements.

A PCM was utilized by Alawadh et al. [14] to assess a building's thermal effectiveness. The thermal efficacy of the suggested roof PCM system was evaluated during regular business hours by comparing the heat transfer flux next to the surface to the case without a PCM. Using a parametric analysis, the effects of the PCM types used and the geometry of the cone frustum was examined. The conical geometry vessel has the best thermal efficacy among the PCMs that have been examined, and n-Eicosane performs the best of all of them. The results show that depending on the kind of PCM and the design of the PCM cone frustum apertures in Figure 2.3, the heat flow at the internal surfaces of the roof might be reduced by up to 39%.

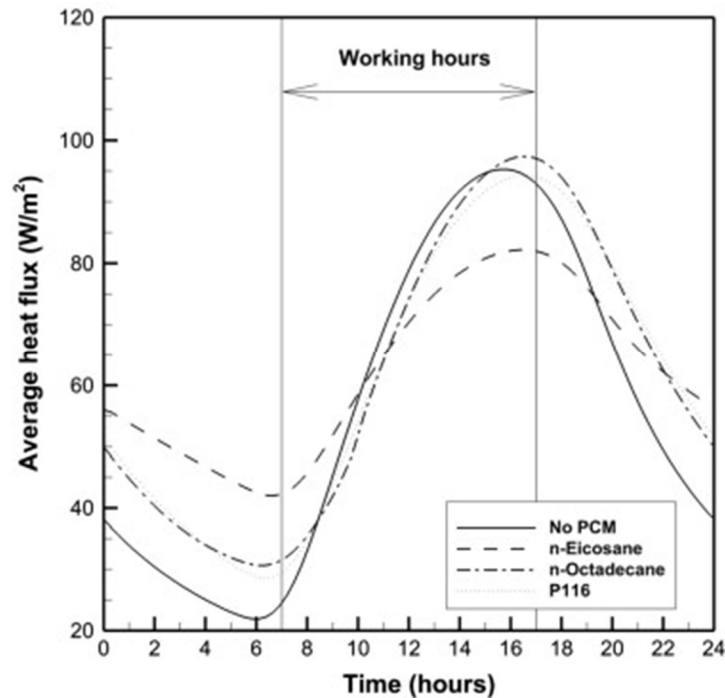


Figure 2.3: Heat flux at the indoor surface for different PCMs [9].

Goia et al. [10] described the thermo-physical performance of a PCM coating in conjunction with clear materials to do numerical studies on many PCM glazing system configurations. Although simulations and experimental data match well on the surface temperature of the glazing, a comparison of simulated and measured transmission irradiances and heat fluxes doesn't often attain the accuracy required. The numerical tool, on the other hand, appears to properly predict the system's thermo-physical behavior, thus it might be a decent initial point for simulations of dissimilar PCM glazing system configurations.

Dubovsky et al. [11] investigated the efficacy of a heat source of the phase change paraffin wax. At 27 degrees Celsius, the wax melts. It was kept as a 20 mm thick layer beneath the floor tile. Temperature fluctuations outside and within were simulated over 24 hours and many days, along with buildup in-wall and heat conduction, surface radiation, inside air natural circulation, and wax solidification and melting. In the structure with windows, the process was evaluated with two cases (with fins, and without fins) at two power factors, and with comparing by windowless

construction. The amount of electricity necessary to maintain thermal relaxation in the structure of a window was 20% greater.

Goia et al. [12] discussed the investigational testing of two samples such as a glazing idea, as well as the evaluation of their energy performance over the summer. Under all boundary circumstances, one of the two designs reduces solar energy gain, though another configuration performs marginally poorer than the model once strong solar irradiation happens. Measurement of thermal transmittances was attempted, and it was discovered that the PCM insertion did not affect the component's U-value. During the summer,

Silva et al. [13] debuted an experimental commercial with a PCM-filled window shutter. The shutter model was built in an outdoors cell with two compartments and south-facing orientation. The heat transfer through the interior wall barriers, inside air temperatures, and outside weather conditions were all monitored and evaluated. The outdoor air temperature varies between 13 and 25 degrees Celsius during the experiment, with mean solar radiation of 237 to 306 W/m². According to the measurements, the compartments with the PCM window shutter have a thermal controlling capability for the internal temperature of 18%–22%. Both of the greatest and lowest temperature maxima decreased by 6% and 9%, respectively. The compartments with PCM enhanced the delay time to achieve the minimum temperature peaks by 45 minutes and the time lag to receive the maximum temperature peak by 60 minutes when compared to the reference compartment.

Baniassadi et al. [14] looked at the thickness of a residential building's insulation and PCM layer. The total cost of the building over the years it has been in use was the fitness function. Particular current worth variables were used to calculate the ideal PCM and insulation layer thicknesses, each accounting for a different scenario regarding the country's economic situation. In all circumstances, the ideal PCM thickness was zero, according to the results. The ideal insulating thickness, on the other hand, varies greatly by area and PWF. The ideal thickness in chilly regions was more than 6 cm, whereas it was almost nil in southern sections of the nation. Furthermore, the findings suggest that, given the country's present economic position, insulating layers were significantly more cost-efficient than phase change materials.

Aditya et al. [15] completed research on the most recent advances in structure thermos insulations, in addition to life round examination and probable emissions reductions through the use of appropriate insulation materials. Liu et al. [16] studied the thermal double glass unit performance occupied by PCM materials of various thicknesses under cold temperatures in Northeast China throughout the winter. The temperature of the inner surface increased by 158.7%, the overall transferred energy decreased by 109.1%, and the transferred solar energy decreased by 86.1 % when the PCM thickness was 50 mm. Based on all features, thicknesses of 12 mm to 30 mm and melting temperatures of 14 °C to 16 °C were suggested in Northeast China.

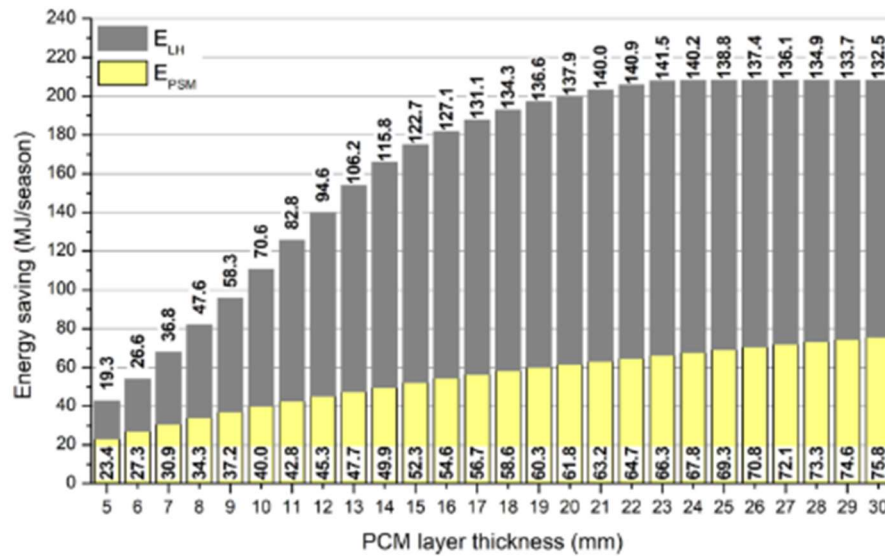
Giovannini et al. [17] investigated the double-glazing unit performance with a PCM layer inserted in it. The PCM visual transmittance in the solid phase was utilized as an input for the simulations, as determined by earlier laboratory observations. The simulations were conducted at several periods throughout the year, including the two solstices and the fall equinox, at various times of the day. The simulations were performed in a chamber with discerning glazing, with a visual transmittance of 0.5, with identical boundary conditions. Daylight Glare Probability (DGP) in two distinct locations in the chamber and spatial useful illuminance was used to assess the visual comfort of the occupants in each scenario. The findings revealed that the glazed package with PCM lets additional sunshine inside the room in most situations, causing a greater glare but lesser spatial beneficial illuminance amounts. On the cooling of an angled solar panel basin solar still,

Kabael et al. [18] examined the impacts of water mass stream rate, PCM, and cover cooling of the inclined solar panel basin solar still (ISPBS). The most distilled water was obtained by freezing the whole surface of the ISPBS glass cover with a fully open water flow, according to the results of the trials. When the minimum mass fraction changes, the glass temperature was higher. The glass temperature was virtually similar to the ambient when the flow cover was entirely opened and the mf was increased from 7.35 to 13.32 kg/h and from 7.35 to 17.72 kg/h. Condensation was accelerated when the glass temperature dropped. Similar to the ISPBS with completely extended cover cooling, the hourly instant efficiency of the ISPBS with fully opened cover cooling was greater than the ISPBS without and with partially covered

refrigeration situations. With partially and completely opened cover cooling, the greatest hour instant efficiency of ISPBSS was determined to be 85% and 88%, respectively. Sari et al. [19] explored the feasibility of structuring dodecyl alcohol (DDA) as an organic PCM for thermal energy storing and the manufacture of activated charcoal from waste tire rubbers. When compared to DDA, the composite PCM's heating and cooling durations were decreased by 17.2 % and 20%, respectively, because of improved thermal conductivity.

Torres-Rodríguez et al. [20] developed a model for calculating heat flow rates through the proposed wall construction and compared the findings to those obtained from complex simulation models often found in commercially available software. The recommended transparent thermal insulation TTI was filled with CO₂ at a pressure of 1000 Pa to test the model since it has a lower heat conductivity than air and argon. The research indicated that the small thermal conductivity gas works by way of a great thermal wall, keeping heat from escaping into the environment. As a result, gases with a lesser thermal conductivity than the gas of CO₂, for example, krypton and xenon, may be utilized with the TTI system.

Tunçbilek et al. [21] observed a PCM layer on an external office wall that was subjected to intermittent cooling. The location, the PCM layer thickness, and the temperature of the phase transition were all adjusted to make the best use of energy investments utilizing latent heat effectively. For the 23 mm layer thickness, energy savings of up to 12.8 % were realized as compared to a single wall case. Each phase conversion temperature over 26 °C lowered energy savings because of the unfavorable effect of latent heat usage as seen in Figure 2.4.



(a) Ventilated office

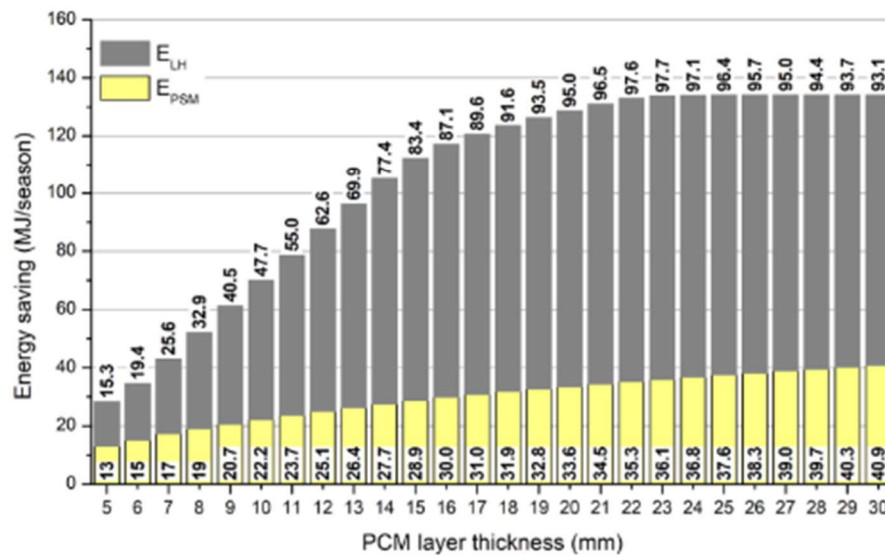


Figure 2.4: Seasonal energy savings as a function of PCM layer thickness [21].

Abbas et al. [22] examined the usage of PCM tablets for insulating material in a hollow element that makes up a wall. To check the effect of PCM with southern walls in the outside normal state, a unique plug type and show walls systems comprising two similar rooms were conceived and constructed. Not only was the mathematical model utilized to validate the results, but it was utilized to study the innovative detailed performance of walls. In order to examine the natural convection inside the room walls, a FORTRAN-based, three-dimensional mathematical model

based on a finite volume arrangement and enthalpy approach was developed. The results of the computational analysis closely matched the experimental measurements. Only a few studies from the previous literature analysis examined the thermal performance of various wall configurations while taking PCM and transparent thermal insulation systems into account. The results show that encapsulating PCM in the treated wall lowers the internal surface wall temperature and the ambient temperature by about 4.7 °C, lengthens the delay time by two hours, lowers temperature fluctuation by 23.84 percent, and results in a decrement ratio of 0.7 when compared to the untreated wall.

Arumugam et al. [28] discussed how to improve the thermal efficiency of buildings in various areas by using the appropriate PCM, insulation, natural, and night ventilation systems. Energy use is significantly reduced in buildings with PCM, insulation, on, natural ventilation, and night ventilation. It was crucial to consider the type of building, its location, weather patterns, ventilation capabilities, and approaches while choosing an effective strategy for a certain building. Finally, insulation integration at the inner building surface has been recommended for climates of Types C and D for a full year in terms of economic benefits and thermal performance, whereas insulation integration at the outer building surface is advised for climates of Types A and B.

The thermal study of the Iraqi construction wall, which was composed of bricks and mortar layers with phase change material (PCM) for use in hot climates, was examined by Abbas et al. [29]. By collecting heat from the bricks during the fusion process before it enters the interior, the PCM was used to lower the temperature. In the model, a composite wall constructed of two layers of mortar and bricks has cylinder holes filled with mortar, PCM, or PCM mixed with nano (TWN) (NTW). The problem was solved through the finite volume method in three-dimensional space. The PCM, as well as the mortar and bricks, were studied using the enthalpy approach. The findings showed that using pure PCM and nano-enhanced PCM would result in peak inner surface temperature reductions of 4.7°C and 4.4°C, respectively. While the usage of pure PCM and PCM coupled with nano resulted in a 2-hour time lag for each.

A parametric analysis of the thermal response of a building wall to a PCM layer for passive space cooling was provided by Sun et al. [30]. Heat flux decreases were employed to investigate the effects of six factors. The following variables were considered: the outside air temperature, the interior air temperature, the amount of insulation, the PCM layer's thickness, its location within the wall cavity, and the temperature at which the PCM phase transition takes place. This was accomplished by developing a numerical model and testing it with experimental data. Within the wall hollow, an optimal PCM layer position range was discovered for each variation between the indoor and outside air temperatures, resulting in more than 50% smaller reductions in heat flux. It was discovered that a first-order parameter determined where the PCM layer was located inside the wall cavity. The ideal position of the PCM layer somewhat migrated toward the exterior wall as the thermal resistance of the wall insulation increased. Figure 2.5 shows that as the PCM layer thickness rose, the peak heat flux decreased to the point where the performance began to suffer. The ideal PCM layer thickness was 7 mm for the cases that were looked at. For better performance during space cooling, the PCM phase transition temperature should be between 27 and 31 °C when the interior air temperature was set at 24 °C.

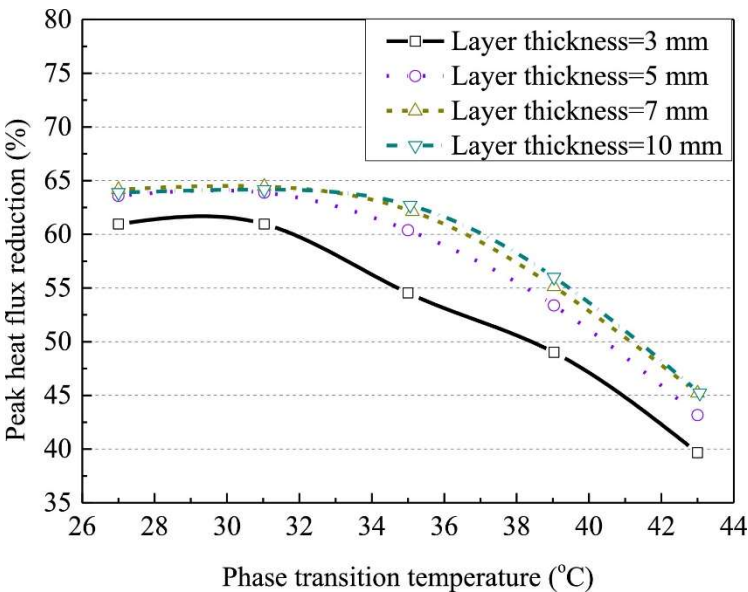


Figure 2.5: Highest peak heat flux decreases for numerous PCM layer thicknesses as a function of PCM phase change temperature and a greatest wall surface temperature of 70 °C [23].

Mustafa et al. [24] employed SP21-EK to reduce the percentage of energy used by structures. Momentum equations with energy were created in this numerical investigation. The focus of this study was on the buildings' interior temperature and its effects, even though several studies have indicated the outside temperature as a crucial factor in the choosing of PCM. The air conditioning system was in charge of regulating the interior temperature, which could be changed as a single or recurring set point. Set points of (21-26) °C were chosen for the first scenario, and it was shown that SP-21EK presence decreased energy consumption by 43.2 percent at the ideal set point (22°C) and by 20 percent at 26°C. The impact of PCM was investigated in conditions of (21-23) °C, (21-24) °C, (21-25) °C, and (21-26) °C. Energy savings from using SP21-EK were 20341, 18164, 15131, and 13160 kWh, respectively. The situation of 21 to 23 °C, which matches to the PCM phase transition from 21 to 23 °C, was determined to have the most beneficial outcomes.

2.2 THE NOVELTY OF THE STUDY

The thermal performance of a PCM with a glass unit was neither experimentally nor statistically investigated for the climate of Türkiye. Numerous experimental articles investigated the heat transfer properties of PCM materials used in glazing units, however numerical analyses using ANSYS software are required to look into the thermal performance of PCM materials. No work has looked into the analysis of equivalent stresses and total deformation caused by temperature for the PCM and glass layers. The impact of temperature on the PCM material's liquid percentage was only briefly examined in a few articles. These points provide a conclusion to the study's objectives:

- a. Numerical study of thermal analysis of PCM material with glass for insulation purpose
- b. The simulation model will be validated by a previous experimental study
- c. Investigation of the influences of PCM thickness on the thermal performance of the setup
- d. Latent heat and liquid volume fractions will be performed

- e. The Turkish climate will be considered in this study
- f. Stress analysis of the PCM material will be introduced



3. NUMERICAL STUDY

The simulation is applied for 24 hours, and the beginning is at 7 am on the highest temperature day of the year in Adana in Türkiye where Adana is the highest ambient temperature city. Various thicknesses of PCM material will be studied to determine the optimum thickness. A numerical study of thermal analysis of PCM material with glass for insulation purposes will be investigated. The simulation model will be validated with a previous experimental study for model verification.

3.1 PHYSICAL DOMAIN

The model for the problem is completed by SOLIDWORKS according to the dimensions of the previous experimental study [16] as seen in Figure 3.1. It consists of three layers (internal glass layer, external glass layer, and PCM layer). The dimensions of the glass layers are 0.5 m in wide and one m in length while the PCM layer has the same dimensions.

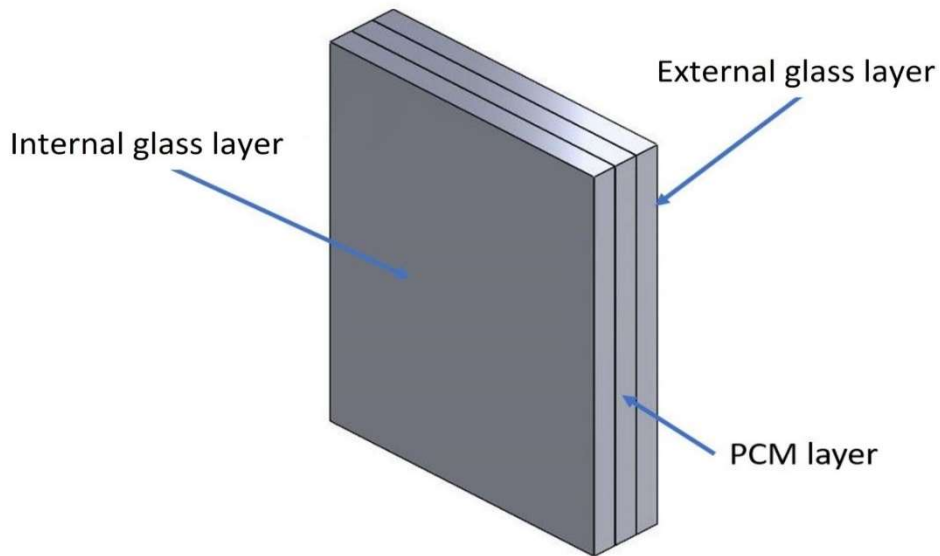


Figure 3.1: Modelling of PCM with glass unit.

The thickness of the two-glass layer is 6 mm. the thermal and optical properties of the PCM and the glass layers are illustrated in Table 3.1. The mass density of the solid and liquid phases are 880 kg/m³ and 770 kg/m³, respectively.

Table 3.1: The thermal properties of the PCM material and glass layer

Material	Thermal conductivity W/m K	Mass density kg /m ³	Specific heat kJ /kg K	Latent heat storage kJ /kg	Melting point temperature
PCM	0.2	770-880	2	250	28 °C
Glass	0.8	2400	0.72	-	-

Table 3.2: The optical properties of the PCM material and glass layer

Material	Absorptivity	Transmissivity	Emissivity
PCM	0.5	0.6	0.25
Glass	0.1	0.85	0.88

The heat is transmitted to the internal layers through conduction after the heat from the external layer has been absorbed by convection and radiation to the surface of the external glass layer, as shown in Figure 3.2. The PCM layer exhibits latent heat transfer from the solid phase to the liquid phase. When additional heat transmits within the PCM layer and subsequently to the internal glass layer, it appears that some heat is reflected in the surrounding area.

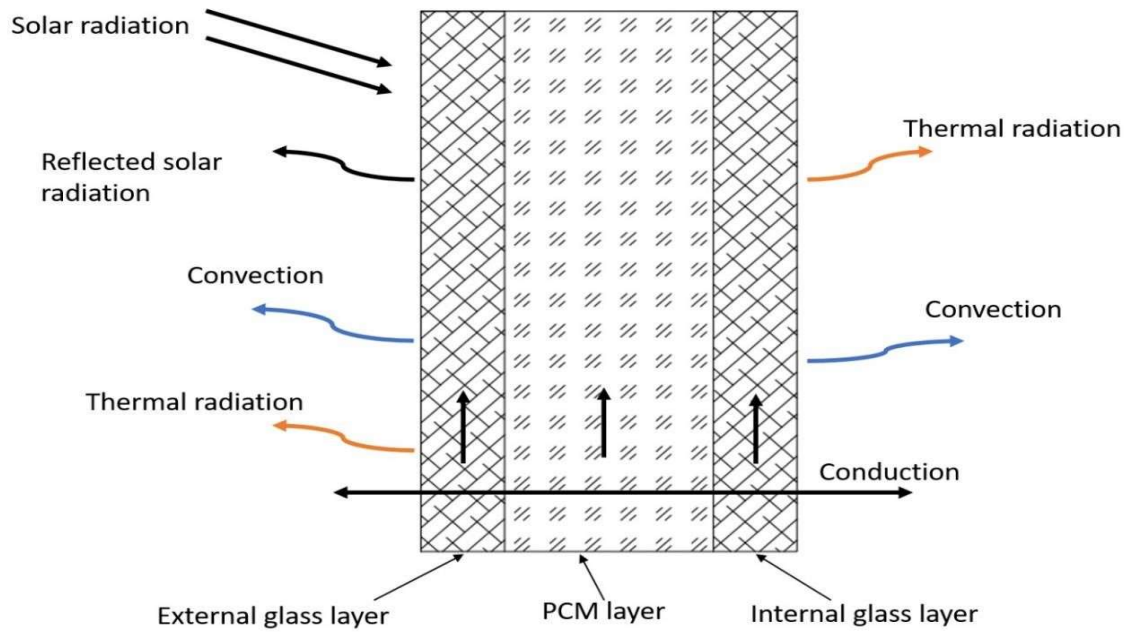


Figure 3.2: Glass layers with PCM layer and heat transfer mechanisms.

To analyze the influence of PCM layer thickness on the glass unit with PCM performance, several thicknesses of the PCM layer (6 mm, 10 mm, 15 mm, and 20 mm) are investigated in Figure 3.3.

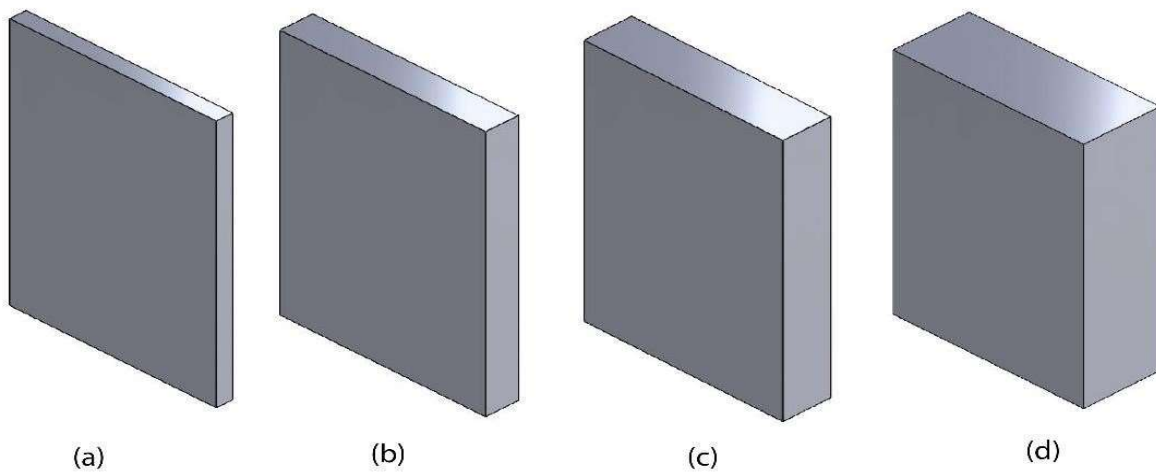


Figure 3.3: Various thickness of PCM layer (a) 6 mm (b) 10 mm (c) 15 mm (d) 20 mm.

3.2 MESH GENERATION

The grid generation for the three-dimensional model of PCM and glass layers, as well as the side view of the model, are shown in Figure 3.4. The computational domain's hexahedron structured meshing was selected for this model. Three different variable meshes, such as 265412, 347251, and 492147 cells, are examined for grid dependence in order to validate the independence of the mesh-generating approach. To verify mesh independence, the temperature measurements from several mesh configurations were compared. The number of 492147 cells was used for the simulation since it is specified that there is no difference in the temperature outcomes between the second and third shapes.

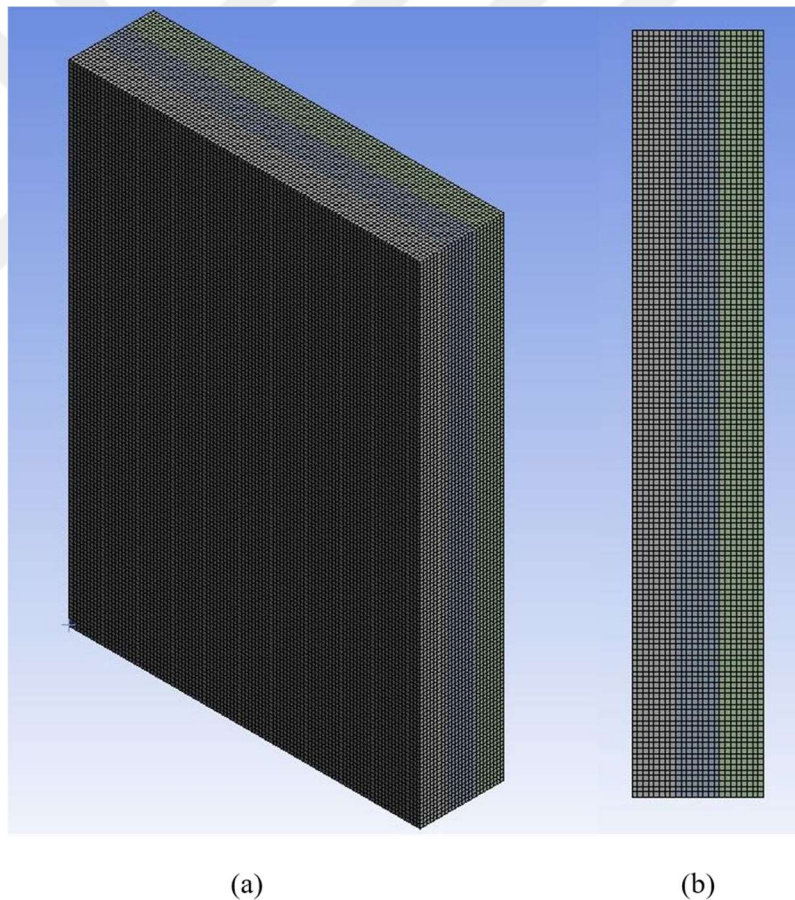


Figure 3.4: Three dimensions and side view of mesh grids.

3.3 GOVERNING EQUATIONS

The nonlinear transient three-dimensional diffusion equation defines a thermal model, which is represented by the heat conduction equation. [16]:

$$\rho \frac{\partial H}{\partial t} = \vec{\nabla} \cdot (K \vec{\nabla} T) + \psi \quad (1)$$

Where ρ is the density in kg/m³,

H is the enthalpy in J/kg,

T is the temperature in Kelvin,

t expresses the time in seconds,

K is the thermal conductivity in W/m·K, and

ψ is the radiative source in W/m³.

The following relationship can be used to determine heat convection and radiation at the interior surface:

$$-K \frac{\partial T}{\partial n} = h_{in}(T_{in} - T_{a,in}) + \sigma \varepsilon (T_{in}^4 - T_{a,in}^4) \quad (2)$$

Where h_{in} is the heat transfer coefficient of the internal surface in W/m²·K,

T_{in} , and T_a , are the internal surface and the internal ambient temperatures, respectively.

σ is the Stefan–Boltzmann constant and ε is surface emissivity.

The heat transported by convection and radiation at the exterior surface can be represented by the following equation:

$$-K \frac{\partial T}{\partial n} = h_{ex}(T_{ex} - T_{a,ex}) + q_r \quad (3)$$

$$-K \frac{\partial T}{\partial n} = h_{in}(T_{in} - T_{a,in}) + \sigma \varepsilon (T_{in}^4 - T_{a,in}^4) \quad (4)$$

h_{ex} is the heat transfer coefficient of the external surface and q_r is the heat transferred by radiation in W/m^2 . T_{ex} is the external surface temperature when $T_{a,ex}$ is the external ambient temperature in the Kelvin unit. Heat flux is defined:

$$\dot{q} = C_p \frac{\partial T}{\partial t} \quad (5)$$

Where C_p is specific heat in $J/kg K$.

Heat Sensible and latent heat (H) of PCM can be calculated by:

$$H = \int_{T_r}^T C_{p,p} dT + \beta Q_l \quad (6)$$

T_r is the reference temperature, β is the PCM liquid fraction, Q_l is the latent heat and where sensible enthalpy of glass in J/kg can be calculated by:

$$Q_l = C_{p,g} T_g \quad (7)$$

By utilizing reverse equation with excel software, governing equation of ambient temperature can be expressed by.

$$T_a = -2 * 10^{-19} t^4 + 2 * 10^{-13} t^3 - 3 * 10^{-8} t^2 + 0.001 * t + 296.9 \quad (8)$$

Where T in Kelvin and t in seconds. By the previous method, the governing equation of total solar radiation that reaches the external glazing can be determined.

$$q_r = -9 * 10^{-20} t^5 + 10^{-14} t^4 - 6 * 10^{-10} t^3 + 10^{-5} t^2 + 0.0043 * t + 114.85 \quad (9)$$

Where q_r in W/m^2 unit and t in seconds. The ambient temperature and solar radiation in Adana city on 29 July 2020 in Türkiye that are utilized in this study are indicated in Figure 3.5 and Figure 3.6, respectively. It can be observed that the maximum temperature was achieved between 1:00 pm and 3 pm.

Equivalent tensile stress, also known as equivalent on-Mises stress, is used to predict the yielding of materials under multiaxial load conditions using the results of simple uniaxial tensile testing:

$$\sigma_v = \sqrt{\frac{1}{2}[(\sigma_{11} - \sigma_{22})^2 + (\sigma_{22} - \sigma_{33})^2 + (\sigma_{33} - \sigma_{11})^2] + 3(\sigma_{12}^2 + \sigma_{23}^2 + \sigma_{31}^2)} \quad (10)$$

The elastic shear modulus can be calculated from the:

$$G = \frac{E}{2(1 + \nu)} \quad (11)$$

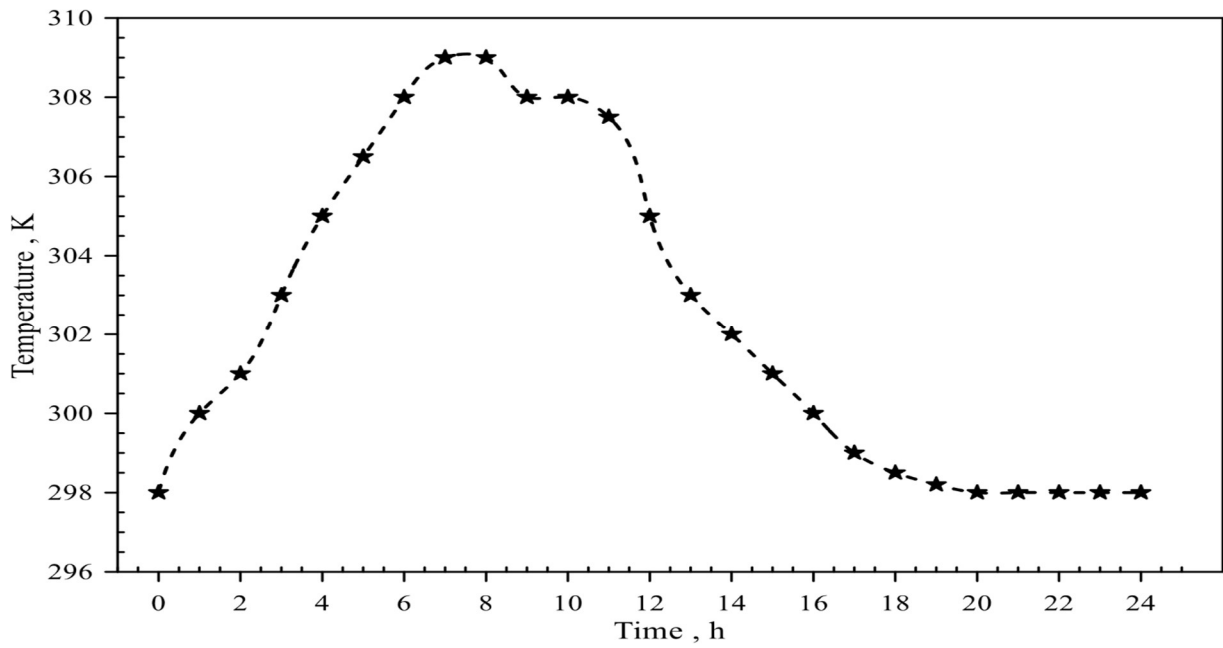


Figure 3.5: Ambient temperature in Adana city on 29 July 2020 [25].

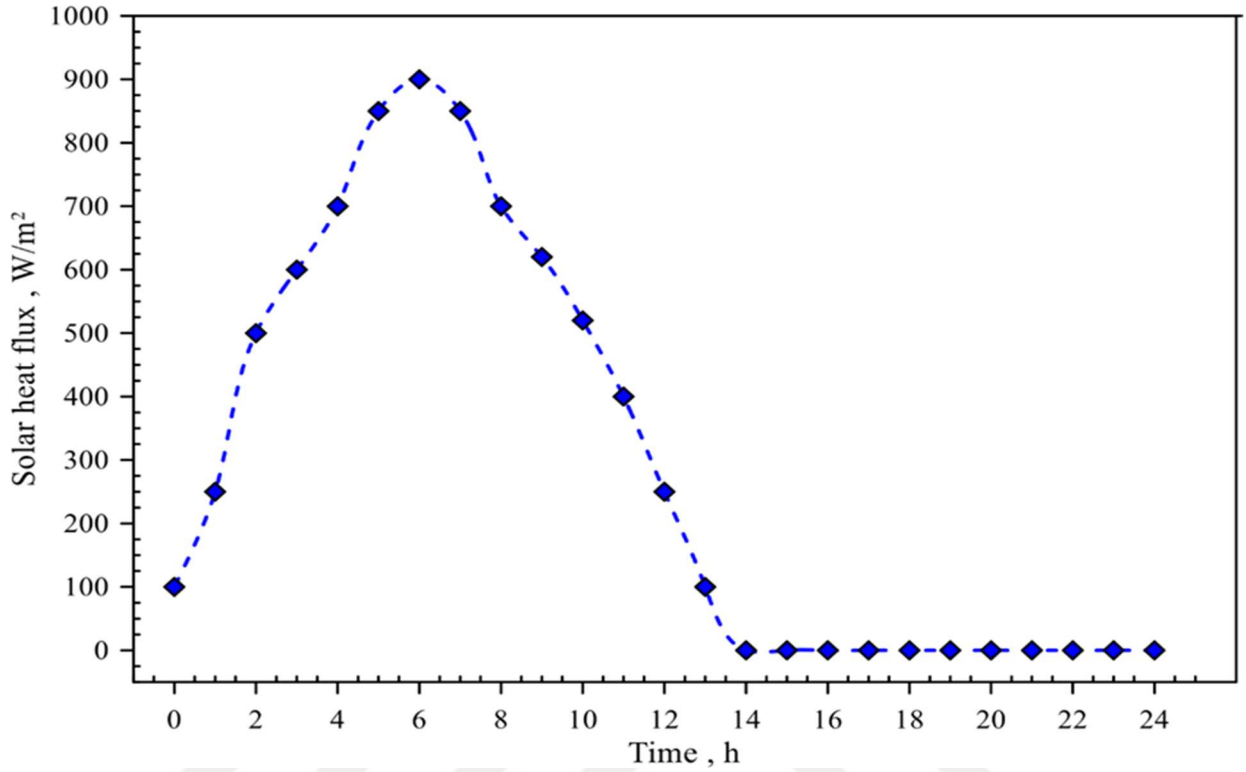


Figure 3.6: Solar radiation in Adana city on 29 July 2020 [25].

3.4 COST ANALYSIS

As the world's population and economy expand, so does the energy demand. Since only roughly 25% of Türkiye's energy needs are satisfied by domestic sources [25], this is very crucial. Saving energy has therefore become necessary. In Türkiye, residential and commercial buildings utilize around 30% of the country's total energy [25]. Therefore, a designer should concentrate on energy conservation in structures [26]. The optimum PCM layer thickness is determined considering the investment cost and the energy cost due to heat transfer from the window. Heat transfer (q) from per unit area through the window is determined according to the:

$$q = U(T_b - T_o) \quad (12)$$

Here U is the overall heat transfer coefficient, T_b is the base temperature and T_o is the mean daily temperature. The cooling energy according to the degree-day method:

$$E_A = \frac{10 * 12 * 30 * 24 * 12 * DD * U}{\eta_s} \quad (13)$$

Where DD is the degree-day sum that can be determined for Adana city [27]. The cooling system efficiency is η_s . The overall heat transfer coefficient (U) of a double-glazed window is defined by:

$$U_D = \frac{1}{(1/h_i) + (t/k_{in, glass}) + (L/k_{PCM}) + (t/k_{out, glass}) + (1/h_o)} \quad (1)$$

Where h_i is the internal heat coefficient and h_o is the external heat coefficient and t is the thickness of the glass which is taken as 6 mm for both single and double-glazed configurations and k_{glass} is the thermal conductivity of the glass.

$$U_D = \frac{1}{(1/9) + (.006/0.8) + (L/0.2) + (.006/0.8) + (1/19)} = \frac{1}{0.179 + 5L} \quad (2)$$

The overall heat transfer coefficient (U) of a single glazed window is defined by:

$$U_s = \frac{1}{(1/h_i) + (t/k_{glass}) + (1/h_o)} \quad (16)$$

So that the annual cooling load for a double-glazed window can be calculated by:

$$E_A = \frac{86400 * DD}{\eta_s} \frac{1}{0.179 + 5L} \quad (3)$$

Considering the lower cooling value of the fuel (LHV), the amount of the annual fuel consumption can be calculated as:

$$m_f = \frac{E_A}{LHV} \quad (4)$$

Natural gas is used for cooling where LHV is equal to 34534500 J/ m³. Assuming C_f is the unit price of the fuel that for natural gas equal to 0.179 dollars per cubic meter according to the universal prices, η_s for systems that used natural gas equals 93%. The annual cooling cost per unit area for a double-glazed window can be obtained as:

$$C_A = m_f * C_f \quad (5)$$

Assuming the lifetime is N years, the total energy cost over the lifetime is converted to the present value by PWF :

$$PWF = \frac{N}{1 + i} \quad (20)$$

Where i is the interest rate (13% in Türkiye).

$$C_c = C_A * PWF \quad (6)$$

The amount of natural gas for the annual cooling energy saving can be calculated by subtracting the annual cooling cost of the double-glazed window from which of the single-glazed window.

The cost of PCM material can be calculated depending on the universal PCM prices [28]:

$$C_{PCM} = \frac{PC}{D} \quad (7)$$

In which C_{PCM} is the PCM cost at time N , the number of years. And it is used for the future predicted price according to the special interest rate of i . The amount of discount factor is introduced as below:

$$D = \frac{1}{(1 + i)^{(N-1)}} \quad (8)$$

4. RESULTS AND DISCUSSIONS

This section looked at the results of using the inverse functions of ambient temperature and solar radiation fluxes with the ANSYS FLUENT program to evaluate temperature and mass fraction. The impacts of various PCM layer thicknesses, including 6 mm, 10 mm, 15 mm, and 20 mm, on the glass unit with PCM are investigated.

4.1 MODEL VALIDATION

In an earlier experimental investigation, Li et al. looked at the impact of PCM's thermophysical properties on the thermal efficiency of a double glass unit packed with PCM. Figure 4.1 compares the external temperatures of the numerical results with that experimental study's external temperatures. The results show that the temperature period delay of the double glass unit with PCM filling improves, and the temperature reduction factor decreases when PCM's density, specific heat capacity, latent heat, thermal conductivity, and melting temperature rise [33]. It can be specified that the nonconformity among the numerical and experimental results is partial. Then, the current simulation results indicate sufficient faithful correctness. The systematic variances among numerical and external temperature previous results for 6 mm thickness are about 2.03%. The maximum difference for external temperature is 5.32% and the minimum difference is 0.92%. The verification findings demonstrated that the disparities across simulation and experimental outcomes are tolerable.

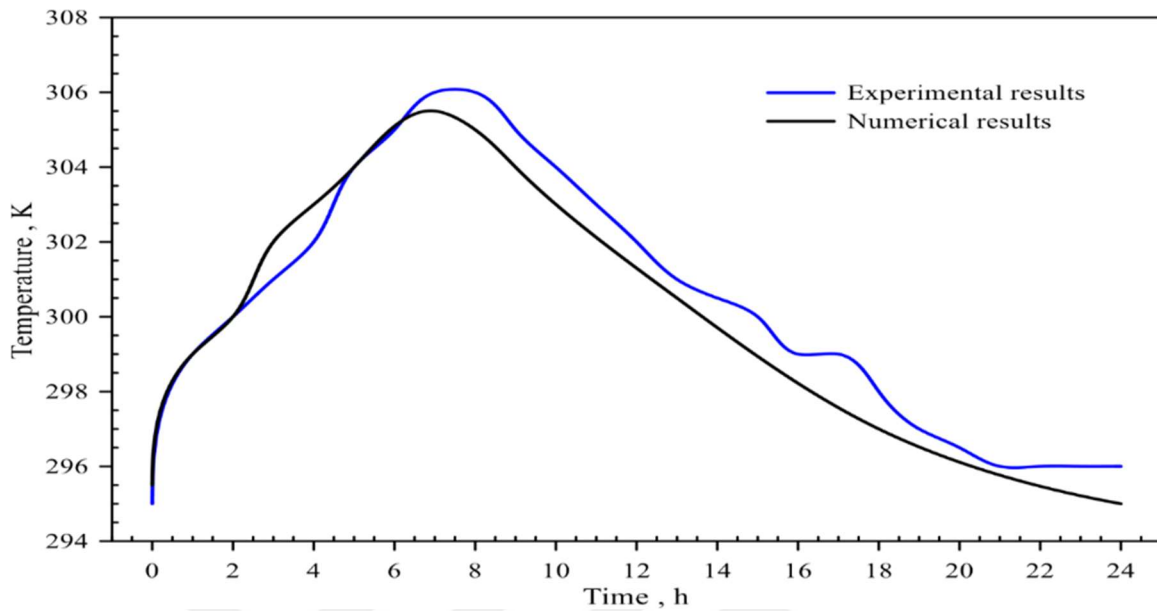


Figure 4.1: Comparing the numerical results of external temperature with a previous experimental study [29].

4.2 TEMPERATURE AND MASS FRACTION

The outer glass external temperatures for different thicknesses (6 mm, 10 mm, 15 mm, and 20 mm) are shown in Figure 4.2 where the temperature decreased with the increase of the thickness of the PCM layer. The thickness of 6 mm achieved the maximum external glass temperature compared to the other PCM thicknesses. It is indicated that the maximum temperature for all the cases was observed at 2:00 pm reaching the figure of 303.5 K. The temperature began to increase at 7:00 am from 296 K to 2:00 pm at 303.5 K then the temperature decreased gradually. It can indicate that the inner glass surface temperature decreases because of enhanced thermal isolation characteristics and improved PCM width. It is indicated that the influence of latent heat enveloped through the layer of PCM appeared in the time lag with the growth of the PCM thickness. The heat flow from solar radiation warmed the PCM layer, which continued to dissolve at which majority of the heat was utilized in PCM melting till the entire layer dissolved, at which point the temperature rose due to sensible heat. The differences in maximum external temperatures between the small thicknesses are small as the PCM layer is transferred from the

solid phase to the liquid phase completely. On the other hand, with the higher thickness, the difference increases so that the heat was utilized only as latent heat.

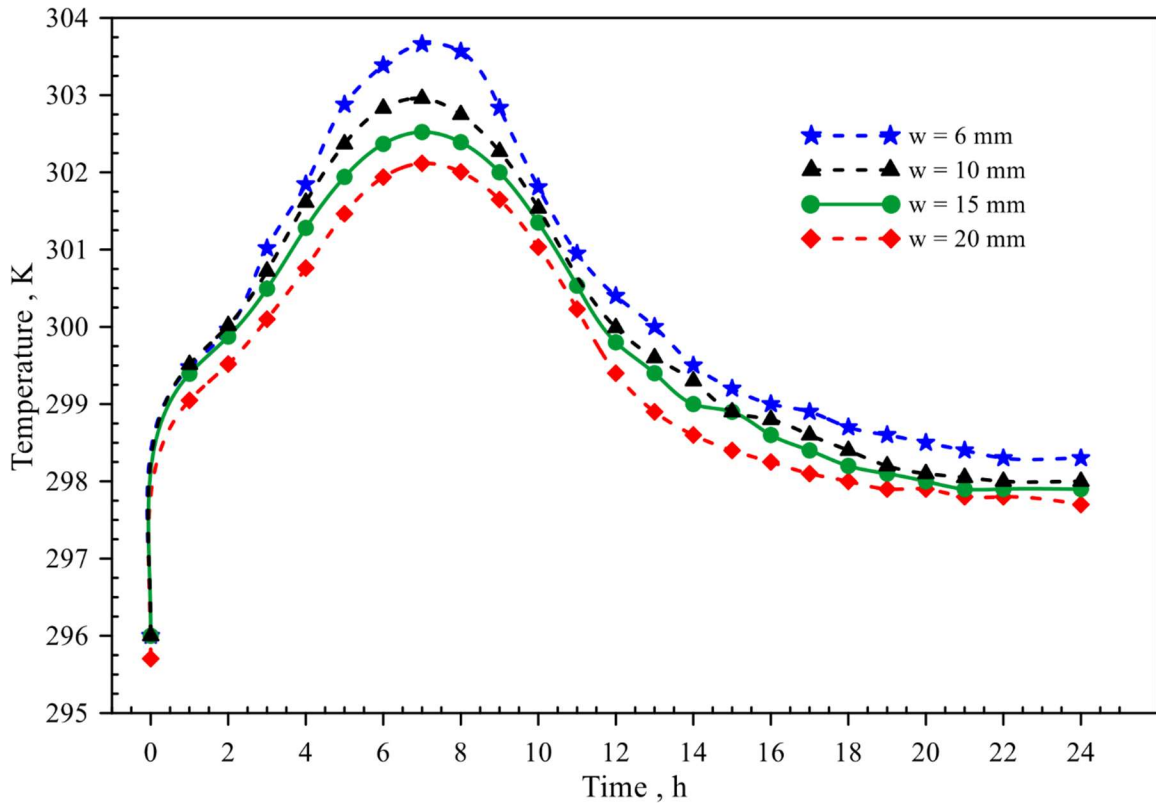


Figure 4.2: External temperature of outer glass for different thicknesses of PCM layer.

The mass fraction that expresses the ratio of the liquid state to the solid state of the PCM layer that is inserted between the glass layers for insulation proposed for one day is indicated in Figure 4.3. It is observed that the PCM layer reached the complete melting at 6 mm thickness case where the 20 mm thickness reached near the half-percentage melting. In the case of 6 mm thickness, the PCM layer began to melt at 7:00 am for some hours until reaching complete melting then the solidification start until all the PCM layers is solidified completely at 11:00 pm. It can be specified that utilizing PCM latent heat is fundamental for the improvement of insulations as this heat consume energy and remains the temperature under control. There are two basic causes for this occurrence. To begin with, the thermal isolation of a glazing unit having

PCM at a thin thickness is poor, resulting in a low glass temperature and a limited liquid fraction of PCM. Second, the absorptivity capability of the PCM sheet at little thickness is low, resulting in low thermal capacity and inefficient use of PCM's latent heat.

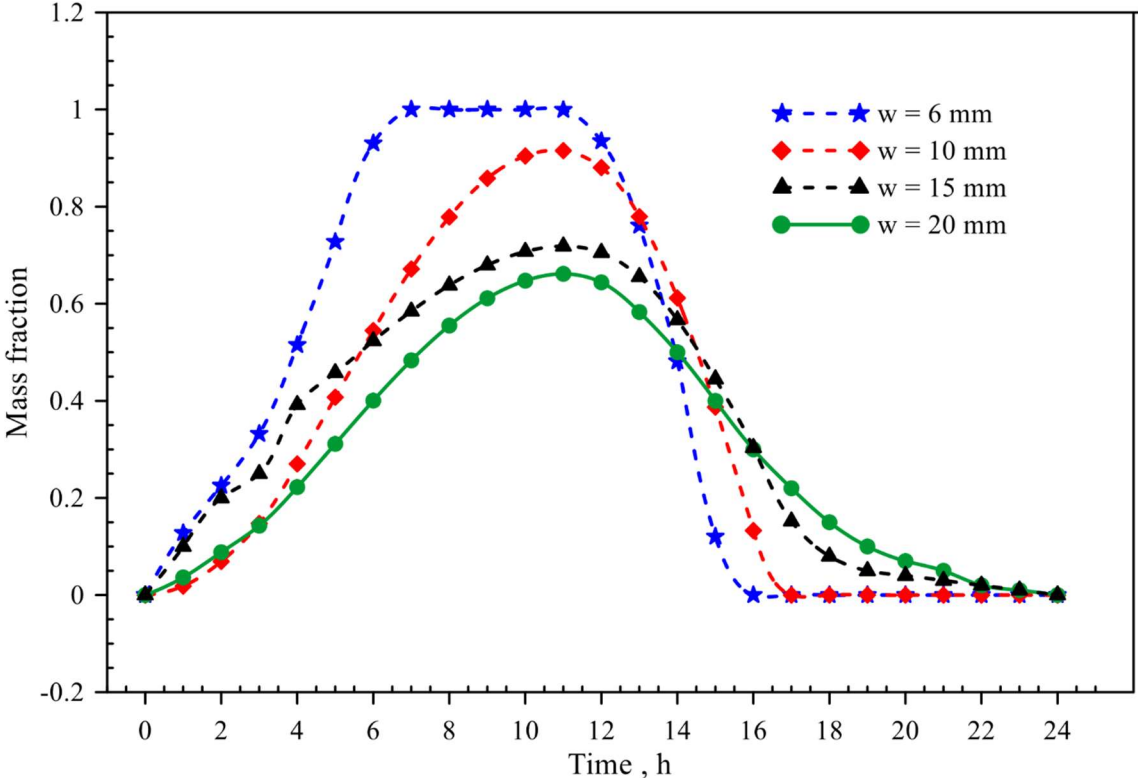


Figure 4.3: Mass fraction of PCM layer for different PCM layer thicknesses.

As shown in Figure 4.4 , Negative energy is sent from the interior to the outside, whereas the overall amount of energy traveling in both directions is positive. The thickness of 6 mm achieved the highest total energy transmitted whereas the 20 mm thickness achieved the lowest energy transport from the warm surface into the cold surface. The total energy transmitted reduced with the growth of the PCM layers' widths.

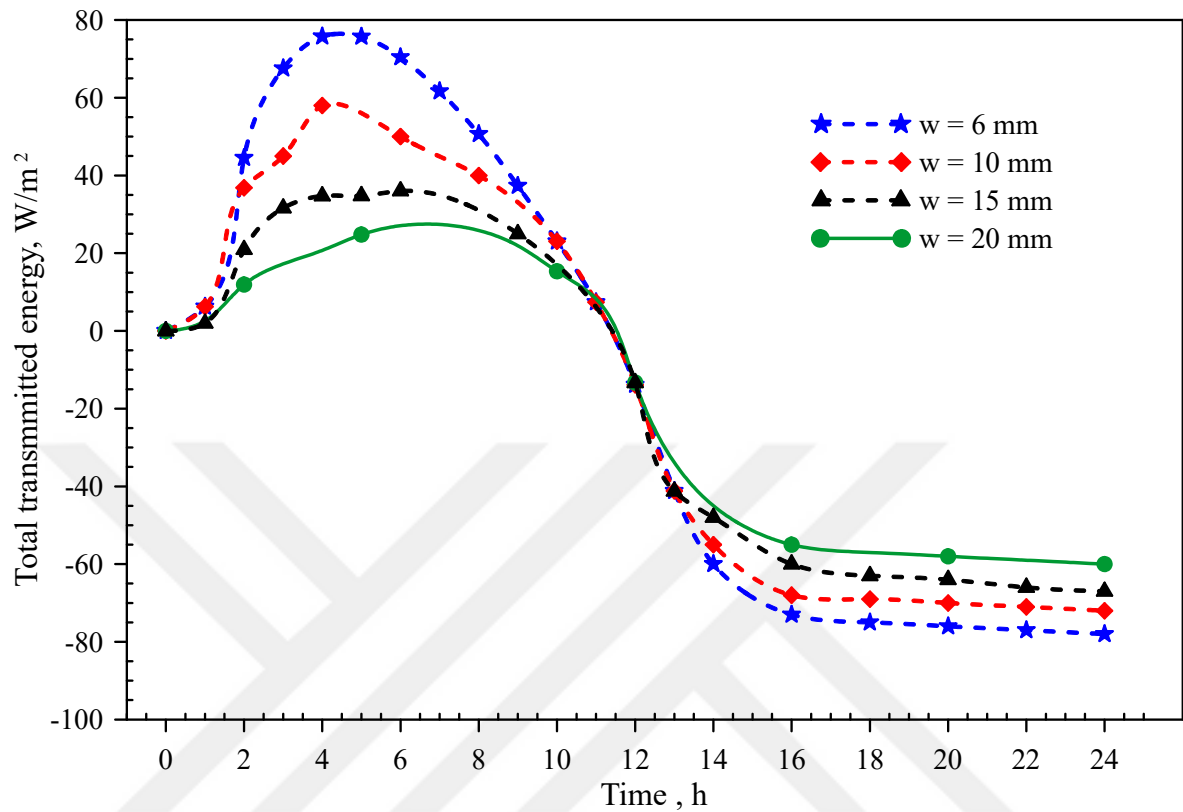


Figure 4.4: Total transmitted energy versus time.

Figure 4.5 shows the temperature distribution contours for the double glass and PCM layer at 10:00 am for each thickness, including 6 mm, 10 mm, 15 mm, and 20 mm. According to the data, the exterior glass temperature drops as PCM layer thickness increases, with 20 mm achieving the lowest external temperature. This can be explained by the fact that the latent heat absorbent layer is 20 mm thicker than in other situations, resulting in the lowest possible exterior temperature.

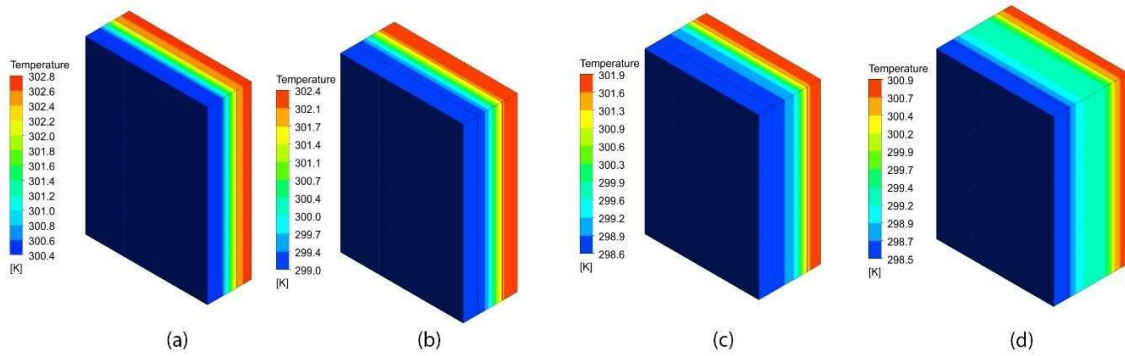


Figure 4.5: Temperature distribution of glass unit and PCM layer at 10 pm for various thicknesses such as a) 6 mm, b)10 mm, c) 15 mm, and d) 20 mm.

Figure 4.6, Figure 4.7, and Figure 4.8 show the temperature distribution contours for the internal layer, PCM layer, and external layer, respectively at 10:00 am for each thickness, including 6 mm, 10 mm, 15 mm, and 20 mm. According to the data, the exterior glass temperature drops as PCM layer thickness increases, with 20 mm achieving the lowest external temperature.

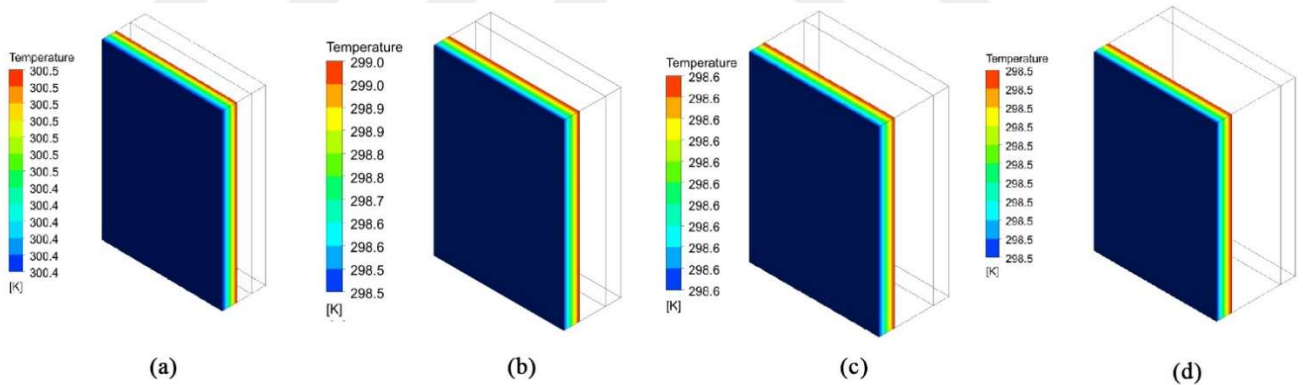


Figure 4.6: Temperature distribution of inner glass layer at 10 pm for various thicknesses such as a) 6 mm, b) 10 mm, c) 15 mm, and d) 20 mm.

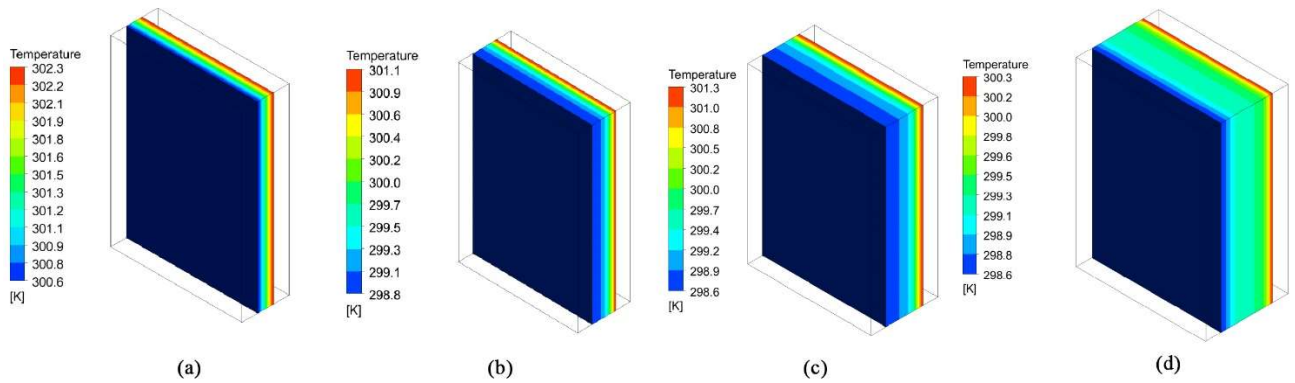


Figure 4.7: Temperature distribution of PCM layer at 10 pm for various thicknesses such as a) 6 mm, b) 10 mm, c) 15 mm, and d) 20 mm.

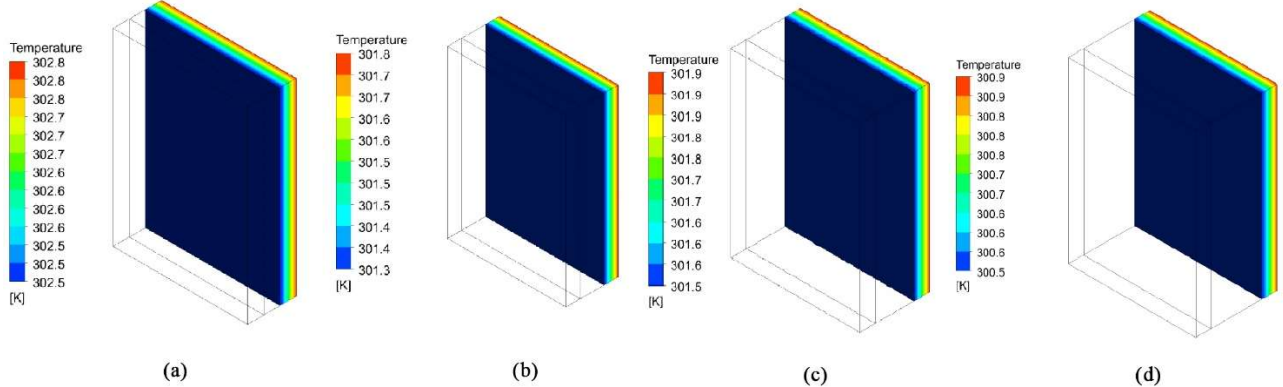


Figure 4.8: Temperature distribution of external glass layer at 10 pm for various thicknesses such as a) 6 mm, b) 10 mm, c) 15 mm, and d) 20 mm.

Melting of the PCM layer is said to begin on the exterior surface and progress progressively within the PCM layer till the entire layer converts to the liquid state. As seen in Figure 4.9. Then the solidification starts smoothly at the outer surface of the PCM layer until the liquid disappears completely from the domain. To obtain the optimum case, comparing the temperatures in all cases of utilized thickness with the economic effects should be performed, the thickness from 10 mm to 15 mm is the optimum choice for the advantages of the smallest temperature. It is indicated that additional thickness can cause a reversed trend for the energy transmitted. The thermal insulation of a glass layer containing PCM at a thin thickness is poor, resulting in a high temperature and a tiny liquid fraction of PCM. A thickness can be useful for thermal insulation,

but it may be non-economical as it uses more PCM layers and the full material doesn't transfer into a liquid fraction. For the 6 mm the external temperature is highest compared to the other configurations where the mass fraction for 20 mm did not extend larger than 0.6 during the day showing that this thickness is not economical for utilizing as insulation material. The influence of solar radiation has appeared with the thickness of 10 mm where the quantity of liquid fraction is higher than the quantity of 20 mm.

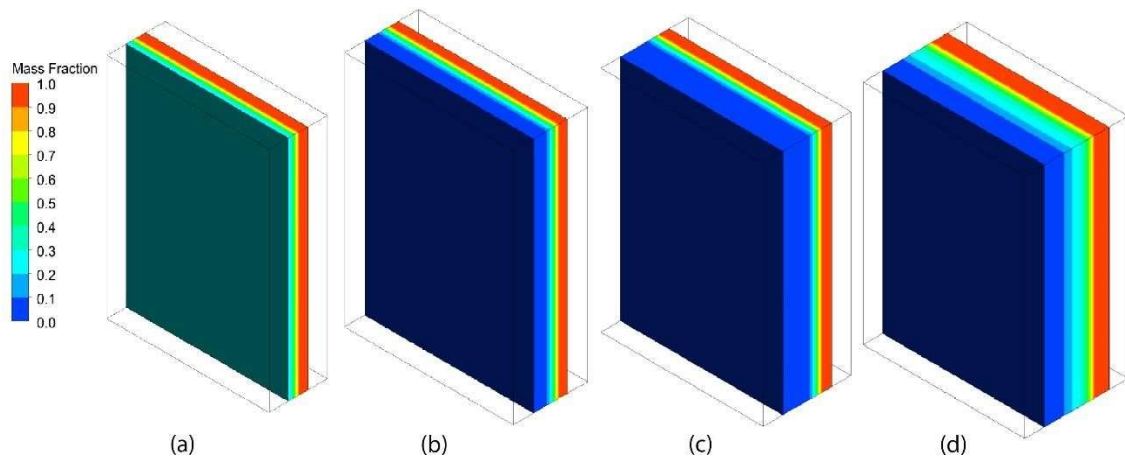


Figure 4.9: Mass fraction distribution at 12 pm for various thicknesses such as a) 6 mm, b) 10 mm, c) 15 mm, and d) 20 mm.

The temperature distribution of the glass layer and PCM layer for 10 mm thickness at several times such as 10:00 am, 2:00 pm, 5:00 pm, and 9:00 pm is illustrated in Figure 4.10. It is indicated that the external surface of the outer glass layer has the maximum temperature whereas the smallest temperature is shown at the surface of the internal glass layer at all times. It can be explained that the maximum temperature is achieved at 2:00 pm following the figure 302.4 K at the external surface compared to other cases. The minimum temperature is indicated at 9:00 pm at the internal surface of the internal glass reaching the number 297.5 K compared with the other times. It is indicated that the effect of solar radiation on the temperature distribution appears at the external and internal surface and the latent heat of the PCM layer influences the temperature distribution.

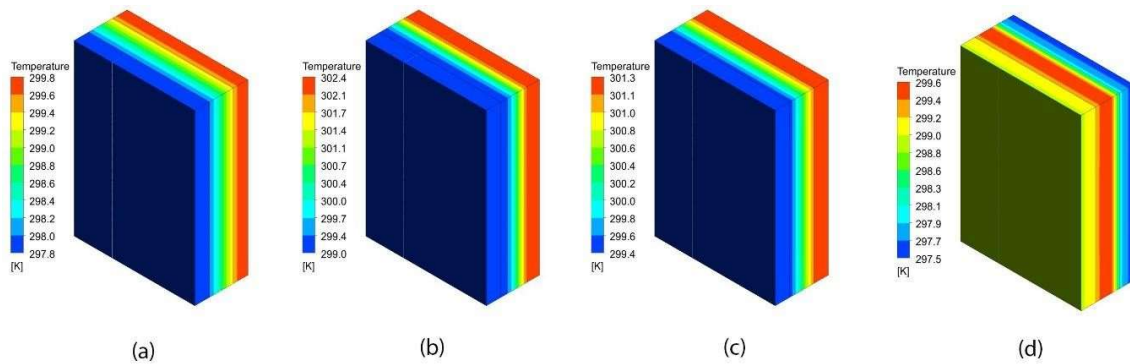


Figure 4.10: Temperature distribution for 10 mm thickness at various times a) 6 mm, b) 10 mm, c) 15 mm, and d) 20 mm.

Figure 4.11 shows the mass fraction of the glass layer and PCM layer for 10 mm thickness at several times such as 10:00 am, 2:00 pm, 5:00 pm, and 9:00. The distribution of mass fraction for 10 mm thickness is chosen as it is the optimum choice for the unit performance. More explanation for the theory of melting and solidifications of the PCM layer can be indicated in this figure. It has been suggested that adding thickness might result in a reversal of the energy-transferred trend. A glass sheet having PCM at a thin thickness has weak thermal insulation, resulting in a high temperature and a little liquid portion of PCM. A thickness could be good for thermal insulation, but this may not be cost-effective because it requires more PCM layers and does not transfer the entire material into the liquid fraction. From the scientific point of view, the previous results can be explained as the increase in thickness of PCM leading to a rise in the thermal resistance of heat transfer and the solar transmittance of PCM can affect the quantity of heat transferred from outdoors indoors. The melting point of PCM affects the time of melting and solidification.

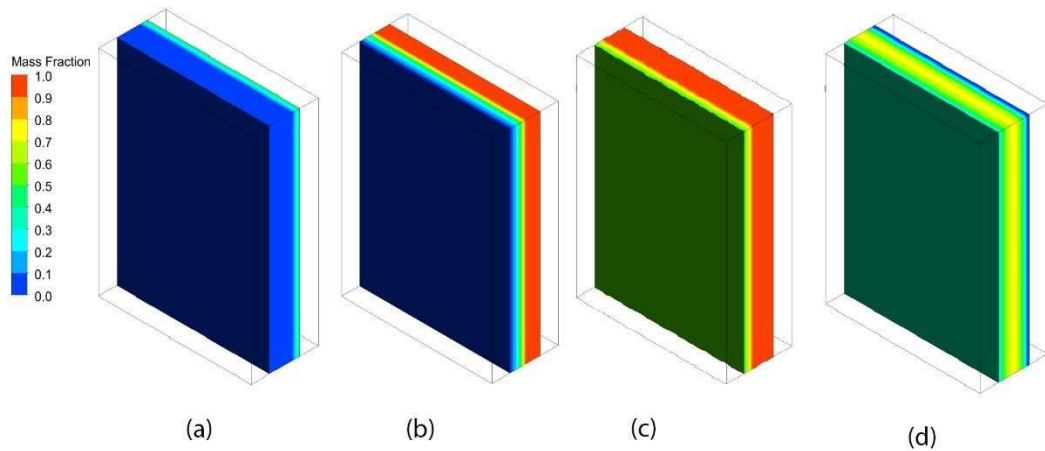


Figure 4.11: Mass fraction for 10 mm thickness at various times a) 10:00 am, b) 2:00 pm, c) 5:00 pm, d) 9:00 pm.

4.3 STRESS ANALYSIS FOR GLASS LAYER AND PCM LAYER

To illustrate the effects of temperature distribution on the equivalent stress and total deformation, transient structure analysis is performed in this section. Figure 4.12 shows the equivalent stress of both glass layers and the PCM layer where can be explained that the external surface of the outer glasses layer was subjected to the maximum stress where the highest temperature is indicated. It is well understood that variations in temperature cause volume changes in any substance.

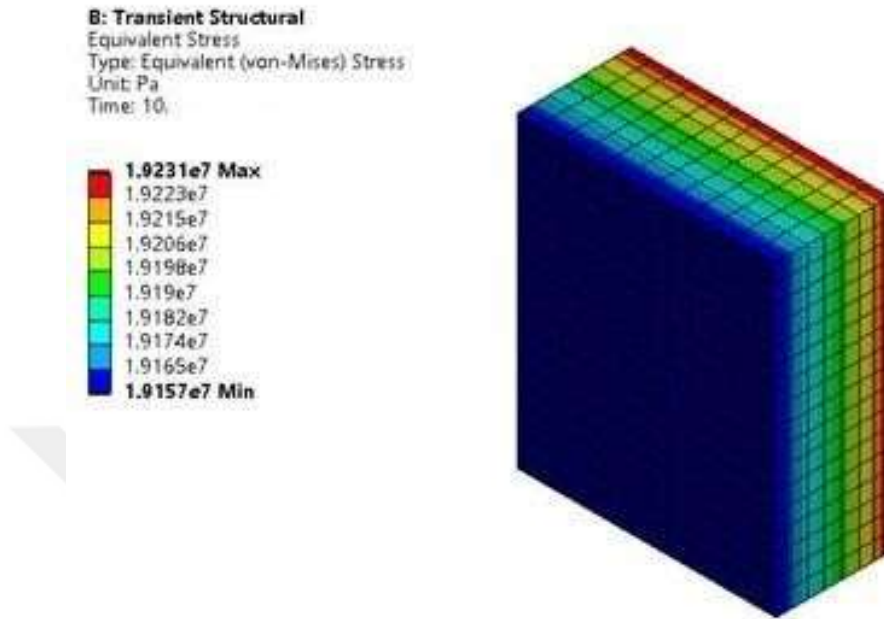


Figure 4.12: Equivalent stress for the glass unit with PCM layer.

The transient structural analysis shows the total deformation of both the glass layer and PCM as seen in Figure 4.13 . The minimum total deformation appeared at the central section of the PCM layer where the maximum is performed at the sides of layers of the glass. The minimum total deformation is near 2.93×10^{-10} m whereas the maximum total deformation is achieved near 3.41×10^{-6} m. The expansion or contraction of a structure is caused by a change in temperature. It can be observed that the equivalent stress of the outer glass has the highest temperature as the change of temperature leads to more structure expansions and this causes higher stress on the surface.

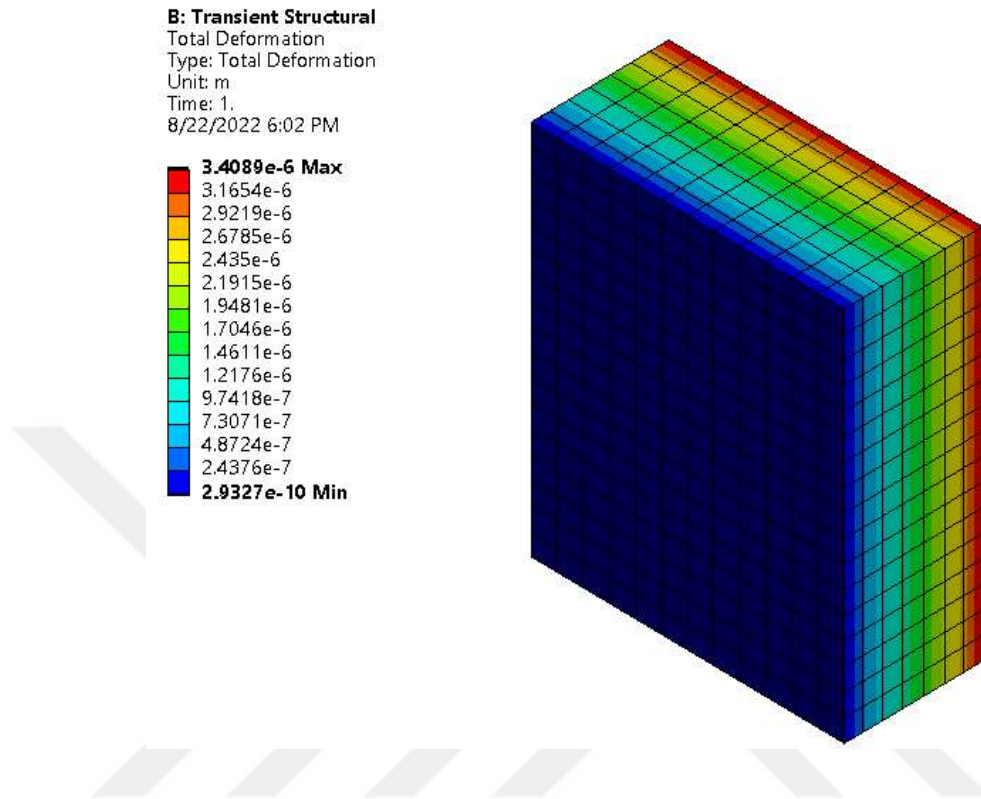


Figure 4.13: Total deformation for the glass unit and PCM layer.

4.4 COST RESULTS

PCM cost, natural gas cost, and total cost versus the PCM layer thickness are investigated in Figure 4.14 for 10 years where the natural gas cost decreases with the increase of PCM layer as the rise of layer thickness increase the thermal resistance of heat transfer inside the building. The PCM layer cost increases with the growth of the PCM layer from 6 mm to 20 mm. that can be explained by the PCM material's rising volume and mass of PCM rise. These results are obtained for Adana city, using natural gas with a PCM layer to increase the insulation. The behavior of the total cost is observed where it decreases with PCM layer thickness from 6 mm to 15 mm then it gradually augmented to 20 mm PCM layer while the PCM layer thickness of the minimum value for the total cost is near 15 mm. It can be concluded that utilizing PCM with PCM layers from 10 mm to 15 mm gives the minimum total cost comparing to the other layers.

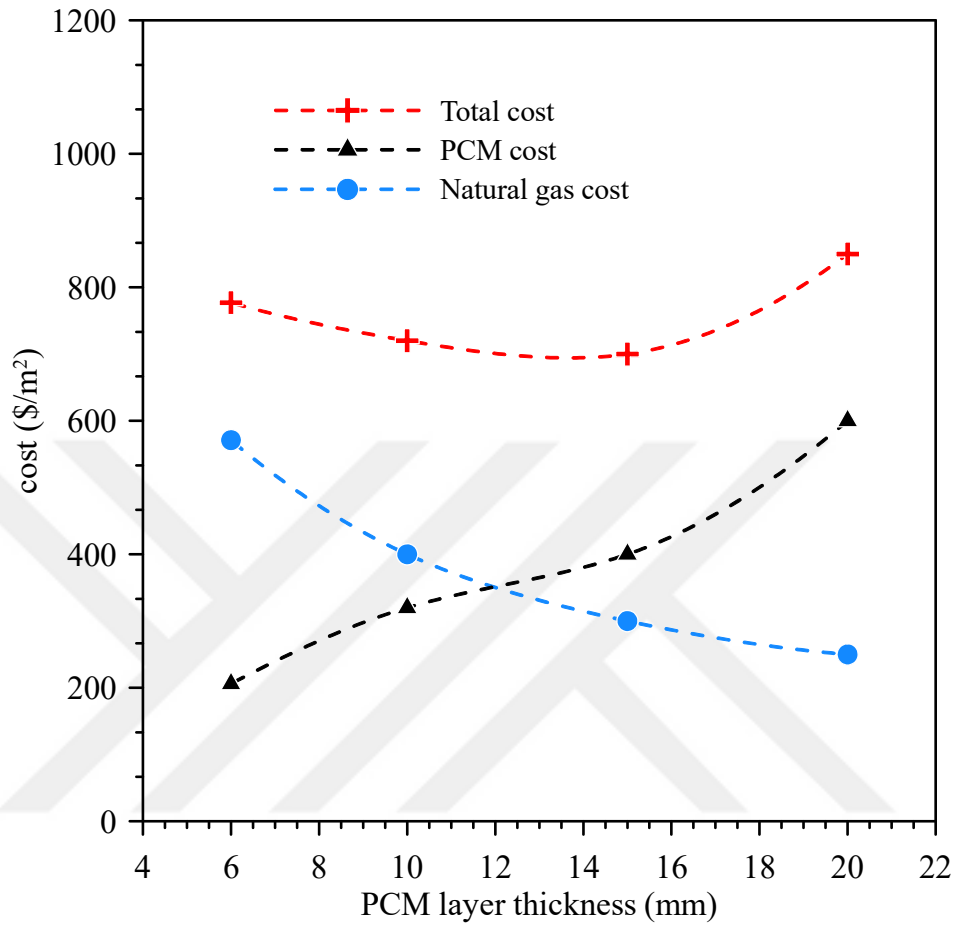


Figure 4.14: PCM cost, natural gas cost, and total cost versus the PCM layer thickness.

The simulation runs are carried out at four different thicknesses: 6, 10, 15, and 20 mm. For verification of the simulation results, the model is validated using prior experimental results [21]. The maximum external glass temperature is noted to be 303.5 K for 6 mm thickness, while the greatest total deformation is 3.40×10^{-6} m. The ideal thickness is reached between 10 and 15 mm, demonstrating the full utility of latent heat. The major findings are summarized in Table 4.1.

Table 4.1: Summary of the results

Case	Value
The thickness of the maximum external glass temperature	6 mm
Maximum temperature time	2:00 pm
Maximum temperature	303.5 K
Complete melting thickness	6 mm
Maximum equivalent stress	1.923×10^7 Pa
Maximum total deformation	3.40×10^{-6} m
PCM optimum thicknesses	10-15 mm

The importance of this study can be concluded in those points:

- a. The goal of this research is to create a strategy for enhancing thermal insulation in buildings using PCM material.
- b. The optimum thickness of PCM was determined to reduce the economic cost and achieve the best performance of two glass layers and the PCM layer unit.
- c. Studying the effects of various thicknesses of PCM is important to indicate the optimum thickness and improve the thermal performance of double glass filled with PCM.
- d. To save on air conditioning costs in the summer in ADANA, Türkiye, it is advised to use PCM material for insulating applications.

5. CONCLUSIONS

A numerical study has been done on the impact of PCM thickness on the thermal performance of a PCM-filled double-glazing unit on the hottest day in Adana, Türkiye. The double glass and PCM layer's thermal and insulating performance is significantly impacted by the thickness of the chosen PCM. From 6 mm to 20 mm, the PCM's thickness rose. These points provide a conclusion about the findings:

- a. As the PCM layer thickness increases, the temperature of the exterior outer glass lowers.
- b. The thickness (20 mm) achieved the minimum external temperature.
- c. It is indicated that even though a thickness might be advantageous for thermal insulation, it might not be economical because it calls for additional PCM layers and doesn't transport the entire material to the liquid fraction.
- d. The minimum temperature is indicated at 9:00 pm at the internal surface of the internal glass reaching the number 297.5 K compared with the other times.
- e. At thicknesses greater than 15 mm, the additional thickness can result in a reversal of the overall energy transferred trends.
- f. The thickness from 10 mm to 15 mm is the optimum choice for the advantages of the smallest temperature for the unit performance.
- g. The minimum total deformation appeared at the central section of the PCM layer where the maximum is performed at the sides of layers of the glass.
- h. The cost of natural gas decreases with the rise of thickness layer where the PCM layer cost increases and the PCM layers from 10 mm to 15 mm gives the minimum total cost comparing to the other layers.

From the scientific point of view, the previous results can be explained as the increase in thickness of PCM leading to a rise in the thermal resistance of heat transfer and the solar

transmittance of PCM can affect the quantity of heat transferred from outdoors indoors. The melting point of PCM affects the time of melting and solidification

The importance of this study can be concluded in those points:

- a. The goal of this research is to create a strategy for enhancing thermal insulation in buildings using PCM material.
- b. The optimum thickness of PCM was determined to reduce the economic cost and achieve the best performance of two glass layers and the PCM layer unit.
- c. Studying the effects of various thicknesses of PCM is important to indicate the optimum thickness and improve the thermal performance of double glass filled with PCM.
- d. In order to save on air conditioning costs in the summer in ADANA, Türkiye, it is advised to use PCM material for insulating applications.

After completing this study, it is advisable to use the PCM for insulation applications and a new material such as Posidonia Oceanica that can be useful also for insulation applications. It is intended to study the thermal properties of Posidonia Oceanica as a composite material and choose the best component of the composite material that can be used with Posidonia Oceanica.

REFERENCES

- [1] M. Pfundstein, R. Gellert, M. Spitzner, and A. Rudolphi, *Insulating materials: principles, materials, applications*. Walter de Gruyter, 2012.
- [2] K. A. R. Ismail and M. M. Gonçalves, "Thermal performance of a pcm storage unit," *Energy Conversion and Management*, vol. 40, no. 2, pp. 115-138, 1999/01/01/ 1999, doi: 10.1016/s0196-8904(98)00042-9.
- [3] K. Ismail, C. Alves, and M. Modesto, "Numerical and experimental study on the solidification of PCM around a vertical axially finned isothermal cylinder," *Applied Thermal Engineering*, vol. 21, no. 1, pp. 53-77, 2001.
- [4] K. Ismail, "Modeling and simulation of a simple glass window," *Solar Energy Materials and Solar Cells*, vol. 80, no. 3, pp. 355-374, 2003/11/01/ 2003, doi: 10.1016/j.solmat.2003.08.010.
- [5] M. Koschenz and B. Lehmann, "Development of a thermally activated ceiling panel with PCM for application in lightweight and retrofitted buildings," *Energy and Buildings*, vol. 36, no. 6, pp. 567-578, 2004/06/01/ 2004, doi: 10.1016/j.enbuild.2004.01.029.
- [6] A. Carbonari, M. De Grassi, C. Di Perna, and P. Principi, "Numerical and experimental analyses of PCM containing sandwich panels for prefabricated walls," *Energy and Buildings*, vol. 38, no. 5, pp. 472-483, 2006/05/01/ 2006, doi: 10.1016/j.enbuild.2005.08.007.
- [7] C. Castellón, A. Castell, M. Medrano, I. Martorell, and L. Cabeza, "Experimental study of PCM inclusion in different building envelopes," *Journal of Solar Energy Engineering*, vol. 131, no. 4, 2009.
- [8] W. A. Miller et al., "Theoretical and experimental thermal performance analysis of building shell components containing blown fiber glass insulation enhanced with phase change material (PCM)," Oak Ridge National Lab.(ORNL), Oak Ridge, TN (United States); *Building ...*, 2010.
- [9] E. M. Alawadhi and H. J. Alqallaf, "Building roof with conical holes containing PCM to reduce the cooling load: Numerical study," *Energy Conversion and Management*, vol. 52, no. 8-9, pp. 2958-2964, 2011/08/01/ 2011, doi: 10.1016/j.enconman.2011.04.004.

- [10] F. Goia, M. Perino, and M. Haase, "A numerical model to evaluate the thermal behaviour of PCM glazing system configurations," *Energy and Buildings*, vol. 54, pp. 141-153, 2012/11/01/ 2012, doi: 10.1016/j.enbuild.2012.07.036.
- [11] V. Dubovsky, G. Ziskind, and R. Letan, "Effect of windows on temperature moderation by a phase-change material (PCM) in a structure in winter," *Energy Conversion and Management*, vol. 87, pp. 1324-1331, 2014, doi: 10.1016/j.enconman.2014.04.007.
- [12] F. Goia, L. Bianco, Y. Cascone, M. Perino, and V. Serra, "Experimental Analysis of an Advanced Dynamic Glazing Prototype Integrating PCM and Thermotropic Layers," *Energy Procedia*, vol. 48, pp. 1272-1281, 2014, doi: 10.1016/j.egypro.2014.02.144.
- [13] T. Silva, R. Vicente, F. Rodrigues, A. Samagaio, and C. Cardoso, "Performance of a window shutter with phase change material under summer Mediterranean climate conditions," *Applied Thermal Engineering*, vol. 84, pp. 246-256, 2015/06/05/ 2015, doi: 10.1016/j.applthermaleng.2015.03.059.
- [14] A. Baniassadi, B. Sajadi, M. Amidpour, and N. Noori, "Economic optimization of PCM and insulation layer thickness in residential buildings," *Sustainable Energy Technologies and Assessments*, vol. 14, pp. 92-99, 2016.
- [15] L. Aditya et al., "A review on insulation materials for energy conservation in buildings," *Renewable and Sustainable Energy Reviews*, vol. 73, pp. 1352-1365, 2017/06/01/ 2017, doi: <https://doi.org/10.1016/j.rser.2017.02.034>.
- [16] C. Liu, Y. Wu, D. Li, Y. Zhou, Z. Wang, and X. Liu, "Effect of PCM thickness and melting temperature on thermal performance of double glazing units," *Journal of Building Engineering*, vol. 11, pp. 87-95, 2017/05/01/ 2017, doi: 10.1016/j.jobbe.2017.04.005.
- [17] L. Giovannini, F. Goia, V. R. Lo Verso, and V. J. S. Serra, "A comparative analysis of the visual comfort performance between a PCM glazing and a conventional selective double glazed unit," vol. 10, no. 10, p. 3579, 2018.
- [18] A. Kabeel, R. Sathyamurthy, S. El-Agouz, E. M. J. J. o. T. A. El-Said, and Calorimetry, "Experimental studies on inclined PV panel solar still with cover cooling and PCM," vol. 138, no. 6, pp. 3987-3995, 2019.

- [19] A. Sari, T. A. Saleh, G. Hekimoglu, M. Tuzen, and V. V. Tyagi, "Evaluation of carbonized waste tire for development of novel shape stabilized composite phase change material for thermal energy storage," *Waste Manag*, vol. 103, pp. 352-360, Feb 15 2020, doi: 10.1016/j.wasman.2019.12.051.
- [20] A. Torres-Rodríguez, D. Morillón-Gálvez, D. Aldama-Ávalos, V. H. Hernández-Gómez, and I. García Kerdan, "Thermal performance evaluation of a passive building wall with CO₂-filled transparent thermal insulation and paraffin-based PCM," *Solar Energy*, vol. 205, pp. 1-11, 2020, doi: 10.1016/j.solener.2020.04.090.
- [21] E. Tunçbilek, M. Arıcı, M. Krajčák, S. Nižetić, and H. Karabay, "Thermal performance based optimization of an office wall containing PCM under intermittent cooling operation," *Applied Thermal Engineering*, vol. 179, 2020, doi: 10.1016/j.applthermaleng.2020.115750.
- [22] H. M. Abbas, J. M. Jalil, and S. T. Ahmed, "Experimental and numerical investigation of PCM capsules as insulation materials inserted into a hollow brick wall," *Energy and Buildings*, vol. 246, p. 111127, 2021/09/01/ 2021, doi: 10.1016/j.enbuild.2021.111127.
- [23] X. Sun, Y. Zhang, K. Xie, and M. A. Medina, "A parametric study on the thermal response of a building wall with a phase change material (PCM) layer for passive space cooling," *Journal of Energy Storage*, vol. 47, p. 103548, 2022/03/01/ 2022, doi: 10.1016/j.est.2021.103548.
- [24] J. Mustafa, F. A. Almeahmadi, and S. Alqaed, "A novel study to examine dependency of indoor temperature and PCM to reduce energy consumption in buildings," *Journal of Building Engineering*, vol. 51, p. 104249, 2022.
- [25] R. Tuğrul Oğulata and S. Noyan Oğulata, "Solar radiation on Adana, Turkey," *Applied Energy*, vol. 71, no. 4, pp. 351-358, 2002/04/01/ 2002, doi: 10.1016/s0306-2619(01)00050-2.
- [26] M. Arıcı and H. Karabay, "Determination of optimum thickness of double-glazed windows for the climatic regions of Turkey," *Energy and Buildings*, vol. 42, no. 10, pp. 1773-1778, 2010/10/01/ 2010, doi: <https://doi.org/10.1016/j.enbuild.2010.05.013>.

- [27] O. Büyükalaca, H. Bulut, and T. Yılmaz, "Analysis of variable-base heating and cooling degree-days for Turkey," *Applied Energy*, vol. 69, no. 4, pp. 269-283, 2001/08/01/ 2001, doi: [https://doi.org/10.1016/S0306-2619\(01\)00017-4](https://doi.org/10.1016/S0306-2619(01)00017-4).
- [28] M. Rezaei, M. Anisur, M. Mahfuz, M. Kibria, R. Saidur, and I. Metselaar, "Performance and cost analysis of phase change materials with different melting temperatures in heating systems," *Energy*, vol. 53, pp. 173-178, 2013.
- [29] D. Li, Z. Li, Y. Zheng, C. Liu, A. K. Hussein, and X. Liu, "Thermal performance of a PCM-filled double-glazing unit with different thermophysical parameters of PCM," *Solar Energy*, vol. 133, pp. 207-220, 2016, doi: 10.1016/j.solener.2016.03.039.